

---

Theses and Dissertations

---

Summer 2011

# Impact of the 2008 Midwestern flood on Gulf of Mexico hypoxia

Aaron L. Gwinnup  
*University of Iowa*

Copyright 2011 Aaron L Gwinnup

This thesis is available at Iowa Research Online: <https://ir.uiowa.edu/etd/1225>

---

## Recommended Citation

Gwinnup, Aaron L.. "Impact of the 2008 Midwestern flood on Gulf of Mexico hypoxia." MS (Master of Science) thesis, University of Iowa, 2011.

<https://doi.org/10.17077/etd.tjsmlr6u>.

---

Follow this and additional works at: <https://ir.uiowa.edu/etd>



Part of the [Civil and Environmental Engineering Commons](#)

**IMPACT OF THE 2008 MIDWESTERN FLOOD ON  
GULF OF MEXICO HYPOXIA**

by

Aaron L Gwinnup

A thesis submitted in partial fulfillment  
of the requirements for the Master of  
Science degree in Civil and Environmental Engineering  
in the Graduate College  
The University of Iowa

July 2011

Thesis Supervisor: Professor Jerald L. Schnoor

Graduate College  
The University of Iowa  
Iowa City, Iowa

CERTIFICATE OF APPROVAL

---

MASTER'S THESIS

---

This is to certify that the Master's thesis of

Aaron L Gwinnup

has been approved by the Examining Committee for the  
thesis requirement for the Master of Science degree in  
Civil and Environmental Engineering at the July 2011 graduation.

Thesis Committee:

\_\_\_\_\_  
Jerald L. Schnoor, Thesis Supervisor

\_\_\_\_\_  
Gene F. Parkin

\_\_\_\_\_  
Craig L. Just

## TABLE OF CONTENTS

LIST OF TABLES .....	iii
LIST OF FIGURES .....	iv
CHAPTER 1 INTRODUCTION AND OBJECTIVES .....	1
1.1 The 2008 Midwestern Flood.....	1
1.2 The Gulf of Mexico Hypoxic Zone .....	1
1.3 Nitrogen Flux in Midwestern Streams.....	2
1.4 Agricultural Land Use in the Midwest .....	2
1.5 Frequency of Data Collection for Accurate Load Estimation .....	4
1.6 Research Objectives.....	6
CHAPTER 2 MATERIALS AND METHODS .....	7
2.1 2008 Difference in Total Nitrogen Flux to the Gulf of Mexico .....	7
2.2 Data Sources and Load Estimation.....	8
2.3 Potential Difference in Area of Hypoxia due to Additional Nutrients .....	9
2.4 Local Nutrient Flux Due to Flooding in Agricultural Watersheds .....	12
2.5 Simple Economic Analysis of Local Nutrient Losses .....	14
2.6 Measuring the Size of the 2008 Gulf of Mexico Hypoxic Zone .....	16
2.7 Frequency of Data Collection for Accurate Load Estimation .....	19
CHAPTER 3 RESULTS AND DISCUSSION NUTRIENT FLUX AND HYPOXIA .....	24
3.1 Measuring the Size of the 2008 Gulf of Mexico Hypoxic Zone .....	24
3.2 2008 Difference in Total Nitrogen Flux to the Gulf of Mexico .....	28
3.3 Nutrient Flux Due to Flooding in Agricultural Watersheds .....	32
3.4 Potential Difference in Area of Hypoxia due to Additional Nitrogen.....	33
3.5 Nutrient Flux Scaling Over a Range of Drainage Areas .....	33
3.6 Agricultural Costs of Flood Scale Nutrient Export .....	35
CHAPTER 4 RESULTS AND DISCUSSION SAMPLING FREQUENCY .....	47
4.1 Optimal Sampling Frequency for Accurate Load Estimation .....	47
4.2 Statistical Analysis of Resampled High Frequency Data Sets .....	47
CONCLUSIONS.....	57
REFERENCES .....	60
APPENDIX A - DATA USED TO MAKE FIGURES 3-6 THROUGH 3-11 .....	63
APPENDIX B – COMPUTER CODE FOR FREQUENCY ANALYSIS.....	70

## LIST OF TABLES

Table 2-1 Number of iterations and samples for each scheme (Raccoon River).....	22
Table 2-2 Number of iterations and samples for each scheme (Mississippi River) .....	22
Table 2-3 The six gaging stations used for this experiment, and their drainage areas .....	23
Table 3-1 2008 nitrogen and phosphorus flux by watershed.....	29
Table 3-2 Top 10 discharge and water yield years for Iowa and the UMRB .....	31
Table 4-1 Data from the sampling frequency experiment (Raccoon River).....	52
Table 4-2 Data from the sampling frequency experiment (Mississippi River) .....	53
Table A-1 Total Nitrogen Data .....	64
Table A-2 Nitrate + Nitrite Data.....	65
Table A-3 Total Kjeldahl Nitrogen Data .....	66
Table A-4 Total Unfiltered Phosphorus Data .....	67
Table A-5 Dissolved Silica Data.....	68
Table A-6 Total Suspended Solids Data.....	69

## LIST OF FIGURES

Figure 1-1. Iowa corn acres vs. CRP acres and corn price per bushel. As the annual average price per bushel (received by farmers) increases, future commitments for enrollment in CRP seems to drop. Fueled largely by growing ethanol production, average monthly corn prices peaked in 2008 at \$4.78 / bushel, which drove corn acres planted (divided by 10 here for comparison) to a record high –since the CRP program began - of 14.2 million acres in Iowa in 2007 .....	3
Figure 2-1. Example input-output for the Scavia model of hypoxic area prediction. The input values on the left generate the dissolved oxygen “sag curve” at the bottom. The downstream distance where average dissolved oxygen returns to above 3 mg l <sup>-1</sup> is taken as the length of the hypoxic plume.....	12
Figure 2-2. MARB watersheds that were analyzed for difference in nutrient flux between flood flow and median flow years. The watersheds were selected based on involvement in the 2008 Midwest US flooding and completeness of water quality data.....	14
Figure 2-3. Local watersheds involved in the 2008 flooding. The circle indicates the approximate area of the 2008 floods. The Maquoketa River Basin was not included in this analysis due to incomplete data.....	15
Figure 2-4. The R/V Pelican is the primary marine research vessel responsible for measuring and assessing the Gulf of Mexico hypoxic zone.....	16
Figure 2-5. Stations and transects assessed by LUMCON to measure the hypoxic zone. The hypoxic plume emanates from the Mississippi River “crow’s foot” at the extreme right side of the image, then flows Westward (leftward) toward Texas.....	17
Figure 2-6. Aaron Gwinnup onboard the R/V Pelican, with the "CTD" array which is deployed to measure multiple water quality parameters simultaneously, as well as take grab samples of the water column at various depths with a rosette of “Niskin” bottles .....	19
Figure 2-7. High frequency (hourly) nitrate load at Sac City, Iowa. A Hach “Nitratex” probe measured concentration by UV spectroscopy, a USGS gaging station provided discharge data.....	20
Figure 3-1. The extent of the near-record-size 2008 Gulf of Mexico hypoxic zone .....	24
Figure 3-2. This crab was swimming on the surface in 150 foot deep water, an indicator of bottom water dissolved oxygen depletion as crabs are traditionally benthic organisms.....	26
Figure 3-3. Bottle nose dolphins swam alongside the research vessel near the east edge of the hypoxic zone, none were observed in the interior of the zone possibly due to reduced abundance of prey.....	26

Figure 3-4. This dead bivalve mollusk and polychaete annelid were the only signs of “life” recovered from sediment samples in the hypoxic zone.....	27
Figure 3-5. The black anoxic streak in this sediment core smelled like sulfide, the cores were used by others to research historical oxygen depletion. ....	27
Figure 3-6. This juvenile squid and fish were netted at the surface. The lights used by nighttime work crews attracted all sorts of organisms toward the vessel, yet no mature non-mammals were ever spotted in the hypoxic zone.....	28
Figure 3-7. May plus June total nitrogen flux from the Mississippi-Atchafalaya River Basin to the Gulf of Mexico, 1980 to 2008. The 2008 flux is shown as the square shape, the median (dashed line) and first and third quartiles (dotted lines) are also shown. Note that this May plus June sum does not include the bulk of the flood load as it likely arrived at these monitoring stations in July.....	29
Figure 3-8. The median monthly total nitrogen (n=28) delivered to the Gulf of Mexico from the MARB was subtracted from the 2008 flux to find the difference that occurred each month. Spring flooding that occurred in the Midwest states from March to June is largely responsible for the peaks visible here in April, June, and July, accounting for approximately one month travel time. The dominant hypoxic area prediction model at the time used May and June total nitrogen flux as an input, which would have missed a significant amount of the Midwestern flood flux. ....	30
Figure 3-9. The Mississippi River hydrograph for Tarbert Landing, MS (the southernmost gaging station before approximately 30% of the flow is re-directed to the Atchafalaya River). The large anomalous peak in late April is primarily from heavy spring rains in the Ohio River basin, the lesser peak at the beginning of July is the floodwater from the June floods centered in Iowa. As the hypoxia prediction model uses the May and June flux near this station, a large portion of the Midwestern flood would not have been included in the predictions.....	32
Figure 3-10. Assuming that the 2008 April + May TN flux from each watershed represents a portion of the May + June TN flux at the Gulf outlets (roughly accounting for travel time), then that same proportion could be applied to the total predicted hypoxic area. Dividing the predicted area of hypoxia that each watershed is represents by the drainage area of the watershed gives a comparative metric of “area of hypoxia per area of watershed. ....	34
Figure 3-11. Corn area hypoxic yield; similar to Figure 3-10 the predicted hypoxic area was proportioned by individual watershed TN flux. In this case the area in each watershed planted in corn during 2008 was used. Of course not all nitrogen flux came specifically from corn fields, however this gives a more accurate qualitative yield depiction than Figure 3-10 because it accounts for the varying corn acreage.....	35

Figure 3-12. Total nitrogen yield scaling. The solid line is a least squares regression of the median flux for non-flood flow years. The dashed line is the flux for the highest flow years (which could be different for each watershed). The dashed, one-dot line is the flux for the second highest flow years, and the dashed, two-dot line is the flux for the third highest flow years. The median values display a more linear relationship than the flood years and all log-log slopes are less than one, the flood year slopes are approximately 11.4% less than the median slope. This indicates that the rate of flux attenuation over increasing drainage area increases for the flood years, and that the flux-increasing effect of flooding is most prominent in the middle range of drainage areas. ....36

Figure 3-13. Nitrate + nitrite yield scaling. The solid line is a least squares regression of the median flux for non-flood flow years. The dashed line is the flux for the highest flow years (which could be different for each watershed). The dashed, one-dot line is the flux for the second highest flow years, and the dashed, two-dot line is the flux for the third highest flow years. The median values display a more linear relationship than the flood years and all log-log slopes are less than one, the flood year slopes are approximately 15% less than the median slope. This indicates that the rate of flux attenuation over increasing drainage area increases for the flood years, and that the flux-increasing effect of flooding is most prominent in the middle range of drainage areas. ....37

Figure 3-14. Total Kjeldahl nitrogen yield scaling. The solid line is a least squares regression of the median flux for non-flood flow years. The dashed line is the flux for the highest flow years (which could be different for each watershed). The dashed, one-dot line is the flux for the second highest flow years, and the dashed, two-dot line is the flux for the third highest flow years. The median values display a more linear relationship than the flood years and all log-log slopes are less than one, the flood year slopes are approximately 9% less than the median slope. This indicates that the rate of flux attenuation over increasing drainage area increases for the flood years, and that the flux-increasing effect of flooding is most prominent in the middle range of drainage areas. ....38

Figure 3-15. Total unfiltered phosphorus yield scaling. The solid line is a least squares regression of the median flux for non-flood flow years. The dashed line is the flux for the highest flow years (which could be different for each watershed). The dashed, one-dot line is the flux for the second highest flow years, and the dashed, two-dot line is the flux for the third highest flow years. The median values display a more linear relationship than the flood years and all log-log slopes are less than one, the flood year slopes are approximately 37% less than the median slope. This indicates that the rate of flux attenuation over increasing drainage area increases for the flood years, and that the flux-increasing effect of flooding is most prominent in the middle range of drainage areas. ....39



Figure 3-16. Dissolved silica (SiO <sub>2</sub> ) yield scaling. The solid line is a least squares regression of the median flux for non-flood flow years. The dashed line is the flux for the highest flow years (which could be different for each watershed). The dashed, one-dot line is the flux for the second highest flow years, and the dashed, two-dot line is the flux for the third highest flow years. The median values display a more linear relationship than the flood years and all log-log slopes are less than one, the flood year slopes are approximately 20% less than the median slope. This indicates that the rate of flux attenuation over increasing drainage area increases for the flood years, and that the flux-increasing effect of flooding is most prominent in the middle range of drainage areas. ....	40
Figure 3-17. Total suspended solids yield scaling. The solid line is a least squares regression of the median flux for non-flood flow years. The dashed line is the flux for the highest flow years (which could be different for each watershed). The dashed, one-dot line is the flux for the second highest flow years, and the dashed, two-dot line is the flux for the third highest flow years. The median values, in general, display a more linear relationship than the flood years and all log-log slopes are less than one, the flood year slopes are approximately 16.6% less than the median slope. This indicates that the rate of flux attenuation over increasing drainage area increases for the flood years, and that the flux-increasing effect of flooding is most prominent in the middle range of drainage areas. ....	41
Figure 3-18. Both the application rate and cost of nitrogen fertilizer has risen sharply since the 'green revolution'. This graph of Iowa data shows the combination as the average April cost of applied nitrogen fertilizer per acre (average of all common forms).....	42
Figure 3-19. LOADEST output of total nitrogen flux for 5 watersheds comprising 63% of Iowa. 95% confidence intervals are shown (dotted lines), as are the 5 year median and first and third quartiles. The median monthly flux was 9,418 MT N, whereas the June 2008 flux was 93,000 MT N (95% CI: 79,000 to 110,000). ....	43
Figure 3-20. Total nitrogen flux for each of the five biggest watersheds in Iowa. The 2008 flux was significantly greater than the 3 <sup>rd</sup> quartile flux in all cases. ....	43
Figure 3-21. Total value of nitrogen and phosphorus exported by watershed. At least 16% of this nitrogen had natural, non-fertilizer origins, nonetheless a significant fraction of applied fertilizer likely ran off over the course of the year.....	45
Figure 3-22. Total nitrogen and phosphorus yields from whole Iowa watersheds during 2008, this is the water-borne flux divided by each drainage area. ....	45
Figure 3-23. Total nitrogen yield from the corn area in each watershed. This is the flux from the entire drainage area divided by only the area planted in corn in each watershed. The nitrogen likely came from many sources, however corn agriculture is the largest non-point source. ....	46
Figure 4-1. Hourly discharge and nitrate concentration on the Raccoon River at Sac City.....	48

Figure 4-2. Hourly discharge and nitrate concentration on the Raccoon River at Jefferson.....	48
Figure 4-3. Hourly discharge and nitrate concentration on the Raccoon River at Van Meter .....	49
Figure 4-4. Logarithmic comparison of discharge to concentration for the Raccoon River at Sac City.....	49
Figure 4-5. Logarithmic comparison of discharge to concentration for the Raccoon River at Jefferson.....	50
Figure 4-6. Logarithmic comparison of discharge to concentration for the Raccoon River at Van Meter.....	50
Figure 4-7. Comparative column chart showing increasing error as sampling interval is increased. The columns themselves are the means of each iteration set.....	51
Figure 4-8. The coefficients of variation for all resampling sets. Note that as the sampling frequency increases, the coefficient of variation increases, but it increases the most for the smallest drainage area and the least for the largest drainage areas. ....	51
Figure 4-9. Log-Log plot of Figure 4-2, this version better shows the dynamics at the lowest end of the sampling frequency spectrum.....	52
Figure 4-10. Seasonal loads generated by sampling every 6 hours. The hourly reference load is represented by the line at 19,700 metric tons - N.....	53
Figure 4-11. Seasonal loads generated by sampling every 12 hours. The hourly reference load is represented by the line at 19,700 metric tons - N.....	54
Figure 4-12. Seasonal loads generated by sampling every 24 hours. The hourly reference load is represented by the line at 19,700 metric tons – N.....	54
Figure 4-13. Seasonal loads generated by sampling every 7 days. The hourly reference load is represented by the line at 19,700 metric tons – N.....	54
Figure 4-14. Seasonal loads generated by sampling every 28 days. The hourly reference load is represented by the line at 19,700 metric tons - N.....	55
Figure 4-15. Seasonal loads generated by sampling every 8 weeks. The hourly reference load is represented by the line at 19,700 metric tons – N.....	55
Figure B-1. INPUT data spreadsheet layout.....	62
Figure B-2. RESULTS data spreadsheet layout .....	63

## CHAPTER 1

### INTRODUCTION AND OBJECTIVES

#### **1.1 The 2008 Midwestern Flood**

Significant flooding occurred in the Midwestern United States, roughly centered in eastern Iowa, during the spring and early summer of 2008. Dozens of stream discharge records were broken and floodplains approaching the 500 year recurrence interval were inundated ultimately causing over \$10 billion in direct damage to crops, buildings, infrastructure and other property (Linhart and Eash, 2010). Although the event was truly devastating to those affected, it has contributed important knowledge for science because freshly fertilized fields were flushed of highly soluble nutrients at a time when fertilizer application rates and corn acreage planted were exceptionally high (USDA-NASS, 2010). As well, the floodwaters arrived at the Gulf of Mexico at the exact time (July) that nutrient induced hypoxia typically forms.

#### **1.2 The Gulf of Mexico Hypoxic Zone**

The hypoxic zone that forms seasonally in the northern Gulf of Mexico at the mouth of the Mississippi and Atchafalaya Rivers has been monitored and measured systematically since 1985 (Rabalais and Turner, 2001). The total size of the zone is impacted by many factors, however nutrient export – especially nitrogen and phosphorus – to the Gulf from the Mississippi River watershed are the dominant factors. While both N and P are critical, limited nutrients, nitrogen tends to be somewhat more limiting in coastal eutrophication processes, and is therefore used in predictive models for Gulf hypoxic models (CENR, 2000; Turner, Rabalais, Justic, 2006). The 2008 hypoxic zone was predicted to be a record size due to increased nutrient and freshwater discharge related to flooding in the upper Mississippi River basin and Ohio River basin (Rabalais, 2008).

### **1.3 Nitrogen Flux in Midwestern Streams**

Some riverine nitrogen flux has natural origins such as atmospheric deposition, microbial fixation and decomposition, etc. Atmospheric deposition is the largest natural source accounting for roughly 16% of nitrogen delivered to the Gulf. In the Mississippi – Atchafalaya River Basin (“MARB”) this fraction is dwarfed by the amount from human activities such as agriculture and urban sources which are responsible for over 70% of the total. Corn and soybean cultivation alone usually accounts for over 52% (Alexander et al. 2008).

The majority of nitrogen lost from agricultural soils is in the nitrate form ( $\text{NO}_3^-$ ), because it is extremely soluble and mobile in water. The chief loss mechanism is by shallow subsurface flow, which is greatly exacerbated by anthropogenic soil drainage efforts such as drainage tiling and ditches (Royer et al., 2004). Numerous studies have demonstrated the very strong correlation between agricultural nitrogen fertilizer application and increased nitrogen concentration in soil pore-water, groundwater, and surface waters (Kanwar et al., 1985; Spalding and Exner, 1993; Schepers et al., 1995).

Hubbard et al. (2011) found that 22% to 30% of the annual total nitrogen load, and 30% to 46% of the annual total phosphorus load from three Iowa rivers prominent in the 2008 floods was exported during just 16 days of the flood. These rivers, including the Des Moines River, the Iowa River, and the Skunk River are among rivers assessed herein that have been implicated for high nutrient flux rates, even during normal flow years. According to Robertson et al. (2009) these watersheds are capable of yielding up to 6900 kg nitrogen and 858 kg phosphorus per kilometer of reach per year.

### **1.4 Agricultural Land Use in the Midwest**

Demand for corn (aka maize, or *Zea Mays* L.) has spiked recently; in 2007 spring corn planting records (since the beginning of the CRP program) were broken nationally, and in Iowa which is the largest producing US state (93.5 million acres in the US, 14.2 million acres in Iowa) (USDA-NASS, 2010). This increase is due in large part to

increased demand from corn-ethanol production and historically high corn prices. The increase in cultivated acreage may come partially from once fallow or retired marginal land that has now become more economically valuable as cropland than “set aside” land (land enrolled in such programs as the Conservation Reserve Program or Wetlands Reserve Program) as demand causes corn commodity prices to increase, see Figure 1-1 (Secchi et al., 2009). An increase in cultivated marginal land may increase the potential for nutrient loss as low lying wetlands, riparian buffers, and grassed drainage ways – which typically sequester nutrients when managed well – are converted to row crop production (Mitsch et al., 2001). Many marginal areas also tend to be vulnerable to flooding due to their low position in the watershed.

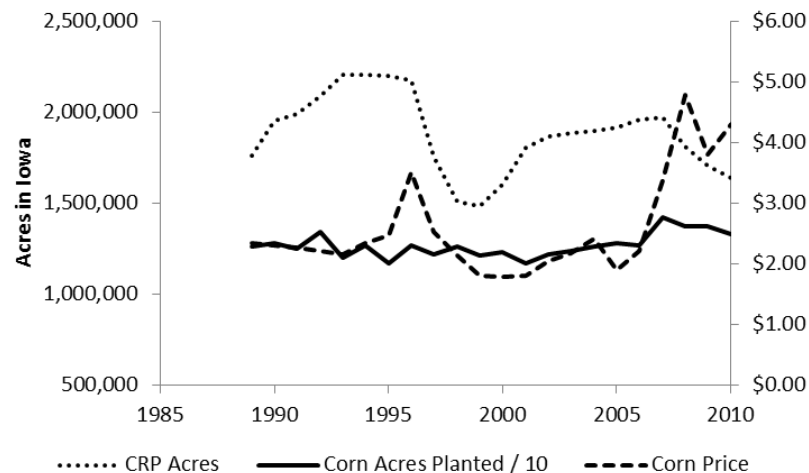


Figure 1-1. Iowa corn acres vs. CRP acres and corn price per bushel. As the annual average price per bushel (received by farmers) increases, future commitments for enrollment in CRP seems to drop. Fueled largely by growing ethanol production, average monthly corn prices peaked in 2008 at \$4.78 / bushel, which drove corn acres planted (divided by 10 here for comparison) to a record high –since the CRP program began - of 14.2 million acres in Iowa in 2007 (USDA, 2010; ISU, 2010)

### **1.5 Frequency of Data Collection** **for Accurate Load Estimation**

The term “nutrient load” in stream and river assessment means the mass of a dissolved or suspended nutrient that passes a particular point on the river in a specified time period. Abstractly, it is calculated as the concentration of the nutrient times the volumetric flow rate of the stream ( $L \text{ [mg/s]} = C \text{ [mg/l]} \times Q \text{ [l/s]}$ ). High frequency monitoring of flow rate is relatively simple and widespread among United States Geological Survey (“USGS”) gaging stations, which are located sporadically along most surface waterways in the US. “High frequency” herein denotes measurements made multiple times per day, sometimes as often as once every 15 minutes.

Monitoring of nutrient concentration is typically done by laboratory analysis of grab samples taken from the stream transect systematically by trained personnel. It would take an unreasonable amount of resources to manually measure nutrient concentration on a high frequency basis at multiple stations, so automatic monitoring devices are sometimes used. These monitors – such as the Hach Nitratax nitrate probe, which uses a split-beam of UV light to estimate nitrate concentration spectrophotometrically – can take readings once every few minutes if desired.

There are however drawbacks to automated probe monitoring. The probes can become fouled or damaged by debris in the water, they need to be re-calibrated regularly, and they can only “sample” one location of the river transect (where they are mounted) so they require an implicit assumption of perfect mixing. For these reasons the data they produce is generally suspected of potential quality issues, and significant pre-processing is required before the data is considered acceptably free of erroneous data points.

One common work-around for the sampling frequency disparity between flow rate (also called discharge) and nutrient concentration is to conduct a statistical regression on the relationship between the two, then apply the regression based correlation coefficients to the high frequency discharge data to produce synthetic estimates of

nutrient concentration – essentially an interpolation of concentration between known points based on changes in discharge. This process is commonly performed with LOADEST, a freeware software application created and distributed by the USGS (Cohn et al., 1992). LOADEST uses the statistical concepts of Adjusted Maximum Likelihood Estimation (“AMLE”), Maximum Likelihood Estimation (“MLE”), and Least Absolute Deviation (“LAD”) as well as several user selectable models of load calculation. Similar to automated probes, the results from LOADEST estimations are also innately questionable as they are the product of a mathematical computation not a direct measurement, and they rely on consistent correlation of concentration to discharge, which is not always the case, particularly with nitrogen concentration (Stenback et al., 2011).

If high frequency data are required for increased accuracy then despite their drawbacks both automated probes and statistical techniques are better than expending resources for high frequency manual sampling. Several questions then arise: Is high frequency data necessary at all? If so, what level of frequency is necessary for each individual monitoring station? How important is the frequency of data acquisition for predicting the impact of each watershed on Gulf of Mexico Hypoxia?

Research by Maclaine Putney has shown that high frequency data collection is more valuable for accurate load calculation as drainage area (and consequently, stream size) decreases because small streams exhibit relatively larger and faster changes in concentration and flow rate than larger streams (small streams are “flashier” than large streams and rivers). For example, a large river such as the Mississippi would not be expected to display rapid changes in chemical composition (as viewed from an Eulerian viewpoint) (Putney, 2010).

The research herein aims to help answer the question: “How frequently does monitoring need to occur to produce reasonably accurate estimates of nutrient loading?” The specific answer will likely be different for every station on every river. This research aims to highlight differences in load estimate quality due to varying sampling frequencies

at stations downstream of a range of catchment areas. The areas range from 700 mi<sup>2</sup> above Sac City Iowa on the Raccoon River, to the bulk of the Mississippi River basin at Baton Rouge, Louisiana.

### **1.6 Research Objectives**

The flooding that occurred in the Midwest United States during 2008, while truly devastating, offered a rare natural experiment that produced data well outside the normal range due to the extreme discharges observed. By expanding the range of documented events, future efforts to model and predict the impact of nutrient flux will be more accurate and insightful as a result. This research may also improve agricultural management decision making in scenarios including increasing meteorological unpredictability due to climate change.

The specific objectives of this research were as follows:

1. Determine the role of the 2008 Iowa flood in Gulf of Mexico hypoxia formation
  - A) Document the increase of nutrient flux due to the flood
  - B) Measure the size of the 2008 hypoxic zone
  - C) Estimate the difference in hypoxic area due to the flood
  - D) Compare flood-scale nutrient flux dynamics to “normal-scale” flux for watersheds ranging in size by orders of magnitude (from small, local rivers to the entire Mississippi River basin)
  
2. Assess the importance of high frequency data collection on determining accurate nutrient loads
  - A) Re-sample high frequency data sets at various intervals and compare seasonal load summations for accuracy
  - B) Compare these results across a range of stream sizes to see if drainage area affects the need for HF data



## CHAPTER 2

### MATERIALS AND METHODS

Existing USGS water quality data collections were utilized to examine patterns in spatial and temporal nutrient flux and areal nutrient yield. By combining the available data with established hypoxic zone areal modeling techniques, differences were inferred regarding the overall impact of flood events on the formation of the Gulf hypoxic zone, and the upstream sources of nutrient flux.

#### **2.1 2008 Difference in Total Nitrogen Flux** **to the Gulf of Mexico**

For prediction and modeling the most important single determinant of hypoxic zone area each year is the spring nitrogen flux. All other relevant parameters were therefore fixed in order to estimate the theoretical areal impact of the 2008 flooding. The May + June total nitrogen load (“TN”, measured approximately 400 km upstream from the Gulf along the Mississippi and Atchafalaya Rivers) was generally used prior to 2009 to predict the size of the hypoxic zone (Scavia and Donnelly, 2007; Turner and Rabalais, 2009). May and June encompass much of the Midwest flooding which occurred throughout spring, but peaked in late June. Allowing for travel time down the Mississippi River (approximately one month from the Midwest), the floodwaters entered the Gulf at the same time that hypoxic plumes typically form each summer. As the peak of flood flow did not likely reach the near-terminus monitoring stations until after June, the full magnitude of flood related nutrient flux may not have been included in areal predictions, which likely makes the predictions herein conservative. Large loadings in April-June occurred in 2008 due to flooding in the Ohio River basin, which also contributes to the Mississippi River basin, and Gulf hypoxia.

For consistency with established methods the May + June total nitrogen load was used to estimate the areal extent of flood related Gulf hypoxia (Scavia, 2003). The net

difference in total nitrogen flux attributed specifically to the 2008 flood was assumed to be the estimated TN flux that occurred during May and June 2008 minus the historical median TN flux for May and June during the preceding 27 years. This difference was used in the prediction model to estimate the potential difference in size of the hypoxic zone.

## **2.2 Data Sources and Load Estimation**

United States Geological Survey Open File Report 2007-1080, updated by Brent Aulenbach et al. in 2008, provides nutrient flux estimates for the Mississippi – Atchafalaya River Basin (or “MARB”) and specific sub-basins from 1973 to 2008. This dataset was chosen as a basis upon which to assess the impact of the flood due to the consistency with which the data were collected and processed, for the significant period of record covered, and for the statistically credible manner in which the data were analyzed. The report consists of multiple data sets summarizing nutrient flux at different stations throughout the MARB. The 2008 version of the report and associated files can be found at: [http://toxics.usgs.gov/hypoxia/mississippi/flux\\_estimates/index.html](http://toxics.usgs.gov/hypoxia/mississippi/flux_estimates/index.html).

The nutrient load data provided in that report was calculated using Adjusted Maximum Likelihood Estimation flux estimates generated by LOADEST, a USGS water quality load integration program. For the MARB as a whole, flow was monitored at Simmesport, LA (Atchafalaya R) and Tarbert Landing, MS (Mississippi R) by the US Army Corps of Engineers, site numbers 03045 and 01100 respectively. Water quality was monitored at Melville, LA (Atchafalaya R) and St. Francisville, LA (Mississippi R) by the USGS and / or USGS approved contractors, station numbers 07381495 and 07373420 respectively.

Flux of biologically critical nutrient parameters were estimated in the report, including mean periodic discharge, nitrate plus nitrite, total Kjeldahl nitrogen (TKN), ammonia, total unfiltered phosphorus, ortho-phosphorus, and dissolved silica (SiO<sub>2</sub>). While not specifically included in the report, TN (total nitrogen) was derived from the

data that were included by summing the nitrate plus nitrite flux with the TKN flux. 95% confidence intervals were also included in the AMLE estimates; as TN was a derived sum, the 95% CI's for TN were summed in quadrature for statistical accuracy. Summing in quadrature means that the difference between each load to be added and its respective upper interval is squared, then the squared differences for the two loads are added, and the square root of that sum is considered the upper interval for the new summed load. The procedure is repeated for the lower interval.

The methods used by the USGS and its contractors for water quality analysis are listed in the National Environmental Methods Index, found on the internet at: <http://www.nemi.gov/apex/f?p=237:1:232094807813256>. The nitrate plus nitrite, TKN, and TN samples analyzed were analogous to “total unfiltered nitrogen”. While collection and analysis techniques, specific parameters monitored, and detection limits have changed over the course of the period of record, appropriate conversions and numerical modifications were incorporated to maintain accuracy (Aulenbach, 2008). The sampling frequency of calibration data (water quality samples) used for nutrient load estimation by LOADEST was monthly, on average. All data points were graded by the USGS as ‘Approved’ or ‘Estimated and Approved’.

### **2.3 Potential Difference in Area of Hypoxia due to Additional Nutrients**

In order to calculate the net difference in the size of the Gulf of Mexico hypoxic zone as a result of 2008 flooding, the same model was employed that was typically used to predict hypoxic zone size in the Gulf of Mexico through 2009. The model (Scavia et al. 2003; Scavia and Donnelly, 2007) was originally developed to determine the amount of reduction in nitrogen loading necessary to meet hypoxia reduction goals. While more complex models have been developed (such as the 3 dimensional model described in Bierman et al., 1994) this simple plug-flow model has been used successfully to reasonably predict the extent of hypoxic zones in the Gulf of Mexico and in the

Chesapeake Bay given variable nutrient loading from point sources (river outlets) (Scavia et al, 2006). Predictions of the Gulf of Mexico hypoxic zone size were based on May and June Mississippi and Atchafalaya River TN flux (as separate systems).

The model used to determine the difference in hypoxic zone size was based on the following established, steady state model (see also Figure 2-1) (Scavia et al, 2003):

$$\begin{aligned} \text{EQN 1:} & \quad B = B_0 e^{-(ax/v)} \\ \text{EQN 2:} & \quad D = [a/(b-a)] B_0 (e^{-(ax/v)} - e^{-(bx/v)}) \\ \text{EQN 3:} & \quad B_0 = W/Q \\ \text{EQN 4:} & \quad \text{Area [km}^2\text{]} = 38.835 \times \text{Length [km]} \end{aligned}$$

Where:

$B_0$  = oxygen demand at the point source [oxygen equivalent mg L<sup>-1</sup>]

$B$  = downstream conc. of decomposing organic matter [oxygen equivalent mg L<sup>-1</sup>]

$D$  = dissolved oxygen deficit [mg L<sup>-1</sup>] [set at 5 mg L<sup>-1</sup> as an average value]

$x$  = distance downstream from the point source [km]

$a$  = first order rate coefficient for organic matter decomposition [d<sup>-1</sup>]

[Actually a parameterization of multiple processes, fixed as 0.003 d<sup>-1</sup>]

$b$  = first order rate coefficient for oxygen influx [d<sup>-1</sup>]

[Actually a parameterization of multiple processes, fixed as 0.01 d<sup>-1</sup>]

$v$  = net downstream advection of subpycnoclinical water [km d<sup>-1</sup>]

[fixed for these calculations at 0.6 km d<sup>-1</sup>, considered conservative] (DiMarco et al. 1997; Rabalais et al. 1999)]

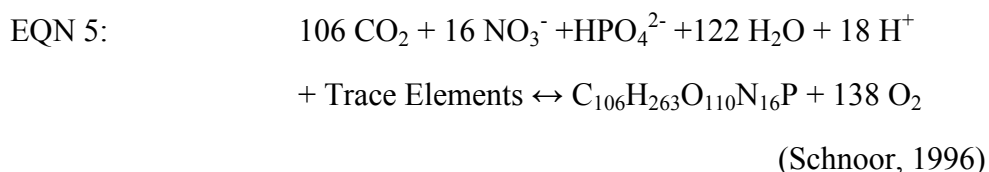
$W$  = point source load of B [g d<sup>-1</sup>]

$Q$  = discharge from the point source [m<sup>3</sup> d<sup>-1</sup>]

This one dimensional model was employed assuming no upstream oxygen deficit, longitudinal dispersion, or oxygen demand ‘legacy effects’, such as sediment oxygen demand and other residual oxygen demand as a result of delayed or diminished decomposition from previously deposited benthic organic matter. Discussion and support of these underlying assumptions was provided in Scavia, et al. 2003. The regression-

based transverse dispersion relationship specific to the northern Gulf of Mexico has been determined for the estimation of hypoxic zone area based on length observations (equation 4) (Scavia and Donnelly, 2007). This linear relationship has been forced through the origin and the  $R^2$  value was found to be 0.8178.

“Length” in equation 4 was found by applying equations 1 and 2 to the Mississippi and Atchafalaya TN loads, and treating these rivers as point sources of nutrient flux. The May + June TN load was summed and divided by 61 days (‘W’ in equation 3) for the 2008 and 27 year median loads (AMLE loads and 95% CI upper and lower bounds). Per equation 3, both of these values were divided by the 27 year median, mean-daily-discharge for May and June, then multiplied by 19.7 g O<sub>2</sub> demand g<sup>-1</sup> N (from the stoichiometry for algae growth and subsequent decomposition, equation 5 below) to produce steady state oxygen demand inputs (Bo in mg l<sup>-1</sup> O<sub>2</sub> equivalent) from each river (Scavia et al., 2003). The Mississippi River input was divided by 2 because roughly half of the river discharges from the “Southwest Passage” which joins the Westward flowing plume, the rest typically flows Eastward from the terminus.



Treating both sources as westward moving plumes, and modeling dissolved oxygen deficit as a plug flow system, a series of two dissolved oxygen “sag curves” were developed. The mouth of the Atchafalaya River is approximately 220 km west of the Mississippi River terminus. Equation 1 was used with  $x = 220$  km to determine the remaining Mississippi River oxygen demand where the two plumes meet. At that point the two oxygen demand values were summed to represent one new plume. Equation 2 was then used to solve for the downstream distance to the point where the dissolved

oxygen deficit returned to a non-hypoxic level. An average dissolved oxygen concentration of  $< 3 \text{ mg L}^{-1}$  was used in this calculation as that level correlates to bottom water hypoxia, which is technically  $\text{DO} < 2 \text{ mg L}^{-1}$  (Scavia et al. 2003). This distance was entered into equation 4 to determine the overall increase in hypoxic zone size due only to increased TN flux.

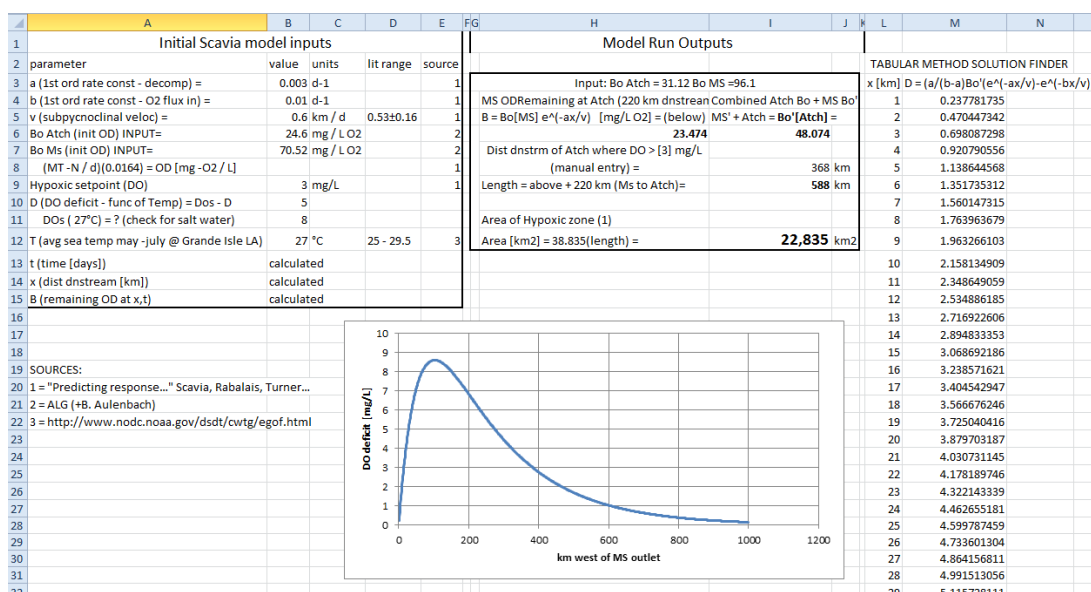


Figure 2-1. Example input-output for the Scavia model of hypoxic area prediction. The input values on the left generate the dissolved oxygen “sag curve” at the bottom. The downstream distance where average dissolved oxygen returns to above  $3 \text{ mg l}^{-1}$  is taken as the length of the hypoxic plume.

## 2.4 Local Nutrient Flux Due to Flooding in Agricultural Watersheds

Nutrient fluxes and yields (“yield” is the flux normalized (divided) by the contributing watershed area) were also compiled to compare spatially normalized differences between normal flow years and flood years in the specific watersheds affected by the 2008 floods. For this purpose “flood years” were assumed to be the years with the top three mean annual discharges for each watershed assessed, and “normal” was

represented by the median of the remaining years in the period of record (usually  $n = 27$  to 34 years, some stations on smaller rivers only began collecting data in 2004, data tables in Appendix A give station specific details).

Some additional nutrient flux information was desired that was not included in USGS OFR 2007-1080, such as total suspended solids flux (“TSS”), and nutrient fluxes from several smaller watersheds in the area affected by the flood. In these cases the methods used for collecting and processing data were similar to those employed for USGS OFR 2007-1080 and all water quality data originated from the USGS at <http://waterwatch.usgs.gov/>.

The effects of localized flooding in a basin as large as the MARB (which covers approximately 3 million square kilometers) tend to become diluted by the time the floodwaters mix with the Mississippi River and then reach the Gulf of Mexico. In order to better analyze the flood related nutrient export and scaling, each sub-basin in the affected area was analyzed for primary nutrient flux. Sub-basins were chosen for this analysis based on involvement in the 2008 flood and continuity of period of record of water quality monitoring data.

As illustrated in Figure 2-2 and Figure 2-3, the specific river stations included were the Iowa River at Wapello, IA; the Skunk River at Augusta, IA; the Des Moines River at Keosauqua, IA; the Wapsipinicon River at DeWitt, IA; the Turkey River at Garber, IA, the Illinois River at Valley City, IL; the Ohio River at Grand Chain, IL; the Mississippi River at Clinton, IA; the Mississippi River at Grafton, IL; the upper Mississippi River Basin as a whole (the “UMRB” is the Mississippi River at Thebes, IL minus the Missouri River at Hermann, MO), and the entire MARB, as described previously. The tables in Appendix A give more information on each watershed, including drainage area, period of record, actual nutrient loads estimated, etc. The nutrient parameters analyzed for flood-scale flux and scaling were total nitrogen, nitrate +

nitrite ( $\text{NO}_3^- + \text{NO}_2^-$ ), ammonia ( $\text{NH}_3$ ), total Kjeldahl nitrogen (TKN), total unfiltered phosphorus (TP), dissolved silica ( $\text{SiO}_2$ ), and total suspended solids (TSS).

### **2.5 Simple Economic Analysis of Local Nutrient Losses**

Much research has been conducted on the origin and fate of surface water nutrients. In 2004, the Iowa Department of Natural Resources published a report that described a mass balance on nitrogen and phosphorus in Iowa soils (Libra et al., 2004). They found that the cycling of nitrogen between the soil, microbes, plants, the atmosphere, and within each of these systems is complex enough that there is of course no way to trace the pathway of nitrogen from one specific source to one specific fate. The focus of our research however was on one specific fate, export via streams and rivers. The mass balance can be divided into open circuits and closed circuits. For example the cycling of nitrogen atoms between soil organic matter and interstitial inorganic matter (principally nitrate and ammonia) was assumed (by Libra et al.) to be a closed loop in approximate equilibrium.

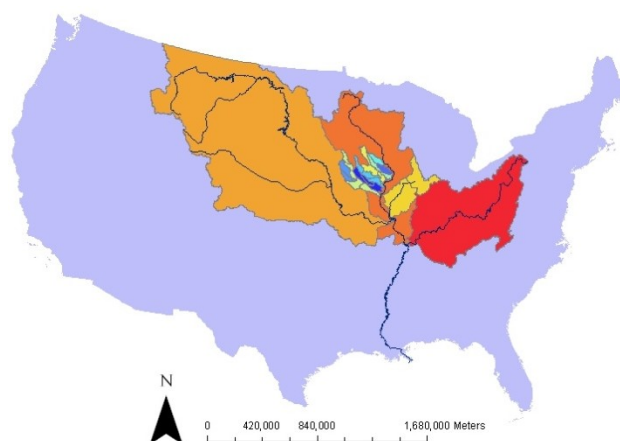


Figure 2-2. MARB watersheds that were analyzed for difference in nutrient flux between flood flow and median flow years. The watersheds were selected based on involvement in the 2008 Midwest US flooding and completeness of water quality data.



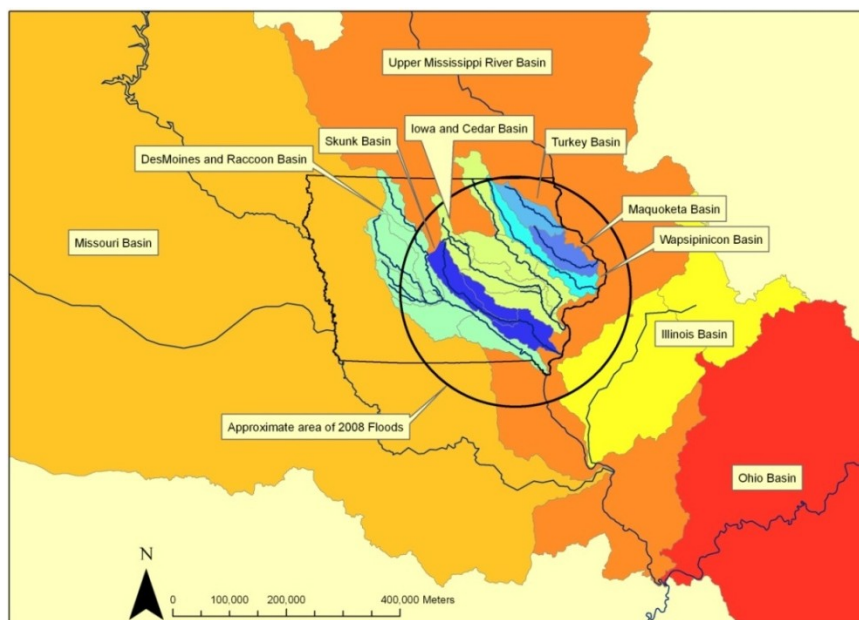


Figure 2-3. Local watersheds involved in the 2008 flooding. The circle indicates the approximate area of the 2008 floods. The Maquoketa River Basin was not included in this analysis due to incomplete data.

Given that the largest variable open loop input to the nitrogen balance is agricultural fertilizer application (Alexander et al, 2008), and that the Libra et al. nitrogen balance found the entire system to be approximately in equilibrium (actually a slight annual loss) so long as fertilizer inputs match the harvest and other outputs, then it seems logical to compare variable fertilizer inputs to the variable outputs observed in local streams, assuming that harvest, grazing, etc. are held constant. This reduction allows the crude yet poignant comparison of economic input factors with ecological output factors and a rough idea of the source-side economic impact of nutrient flux, tangible at the per acre scale. Support for this analytical simplification (the correlation of fertilizer application rate and surface water nutrient concentration) comes from extensive research by others (Turner and Rabalais, 1991; Howarth et al., 1996; Goolsby et al., 1999).

Nutrient yields were calculated by dividing the LOADEST produced flux estimates by the contributing drainage area, as listed by the USGS (accessible at:

<http://waterwatch.usgs.gov/classic.php>). The cost per pound of field-applied nitrogen and phosphorus fertilizer was obtained from the USDA, Economic Research Service (USDA-ERS, accessible at <http://www.ers.usda.gov/Data/FertilizerUse/>, Table 7). The costs for each form of N or P listed were stoichiometrically normalized, then averaged among the forms to produce average costs per pound of each nutrient. These costs were then multiplied by the LOADEST generated fluxes to give estimates of the value of the nutrient losses from each watershed. These results are intended to provide a quantitative picture of the economic side of the loss to complement the mass-wise quantification.

## **2.6 Measuring the Size of the 2008**

### **Gulf of Mexico Hypoxic Zone**

An expedition was mounted July 20 – 28, 2008 to measure the size of the hypoxic zone that typically forms on the north continental shelf of the Gulf of Mexico (off the south shore of Louisiana and Texas). This research was performed in collaboration with Nancy N. Rabalais, PhD, the Executive Director of the Louisiana Universities Marine Consortium (“LUMCON”), and R. Eugene Turner, PhD, of Louisiana State University. The R/V Pelican, a marine research vessel owned by LUMCON (Figure 2-4), is outfitted with extensive water quality sampling and monitoring equipment and was chartered in 2008 specifically for the task of measuring and assessing the hypoxic zone.



Figure 2-4. The R/V Pelican is the primary marine research vessel responsible for measuring and assessing the Gulf of Mexico hypoxic zone. (Image by LUMCON)

Measuring and assessing the hypoxic zone consisted of navigating a series of transects across the area that typically experiences hypoxia each summer. This area has been systematically measured by researchers at LUMCON since 1985, and specific monitoring stations placed along specific transects have been developed over the course of the continuing research (Figure 2-5). The assessment began at the Mississippi River outlet, the research vessel then travelled either north or south along each transect, stopping at each station to deploy instruments, collect data, and collect water and sediment samples. The transect was considered complete when no hypoxia was detected (all measurements reported that dissolved oxygen was  $>2$  mg/l, vertically along the entire water column), at which point the vessel moved west to the next transect. This pattern was repeated 24 hours per day (by two shifts of researchers) until no hypoxia was detected along an entire transect. The last transect to exhibit hypoxia was considered the western edge of the hypoxic zone.

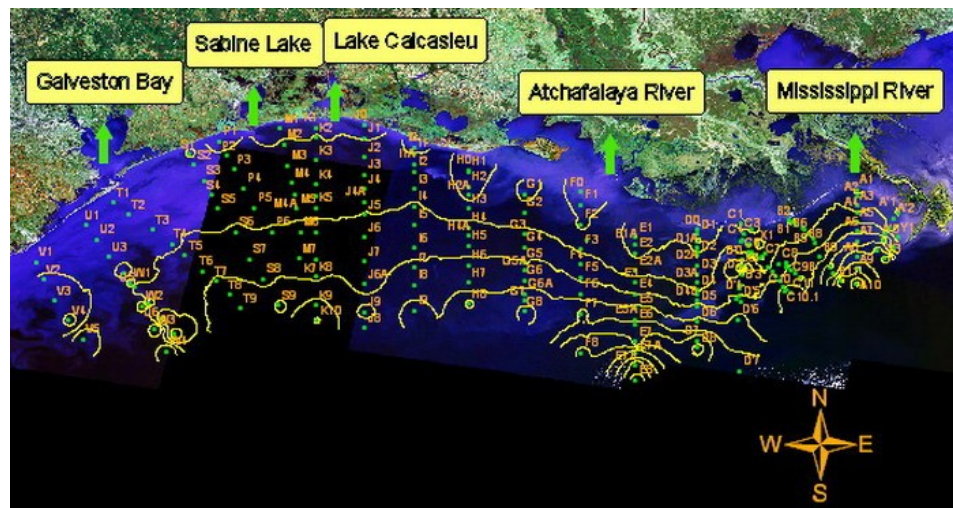


Figure 2-5. Stations and transects assessed by LUMCON to measure the hypoxic zone. The hypoxic plume emanates from the Mississippi River “crow’s foot” at the extreme right side of the image, then flows Westward (leftward) toward Texas. (image from [www.gulfhypoxia.net](http://www.gulfhypoxia.net))

At each station a series of activities was performed to gather data and samples. Among other activities, a bucket on a rope was thrown overboard to collect a surface water sample, and a custom equipment array called a “CTD” was lowered along the water column to the sea floor (originally the device measured only conductivity, temperature, and density, thus “CTD”). The CTD (visible in Figure 2-6) is a negatively buoyant chassis equipped with 12 “Niskin” bottles in a rosette pattern and dual digital sensors for each of: pressure, temperature, conductivity, GPS, dissolved oxygen, optical transmission, optical backscatter, fluorescence, photosynthetically available radiance, and sonar altimetry (Niskin bottles are essentially hollow tubes that snap shut on both ends when triggered, to allow remote sampling of the water column). During lowering of the CTD, a researcher triggered the closure of the Niskin bottles at specified depths, depending on the overall water depth at that location. An additional Niskin bottle was also deployed on a cable to collect a water sample directly above the seafloor.

Upon retrieval of the bucket, CTD, and bottom Niskin bottle the vessel would move on to the next transect while researchers processed the samples for storage and analysis. All electronic data gathered by the CTD was automatically stored on onboard hard drives. All water samples from the bucket and Niskin bottles were processed appropriately for later analysis (the samples were analyzed for suspended solids concentration, assorted nutrient concentrations, chlorophyll-a, and phaeopigments). Most of the assessed parameters were used for aspects of hypoxia research that is unrelated to the research herein. The critical parameter for this research was the spatial extent of the hypoxic zone as a whole, indicated by the extent of bottom-water dissolved oxygen concentration below 2 mg/l.



Figure 2-6. Aaron Gwinnup onboard the R/V Pelican, with the "CTD" array which is deployed to measure multiple water quality parameters simultaneously, as well as take grab samples of the water column at various depths with a rosette of "Niskin" bottles

### **2.7 Frequency of Data Collection** **for Accurate Load Estimation**

Nutrient loads are calculated as the concentration of a constituent multiplied by the rate of volumetric discharge of a stream or river. The values of these two parameters are not known on a continuous basis though. If measurements are taken once per hour, then those values are assumed to represent the interim hour before another sample is taken, likewise if measurements are only taken once per day, or per month. Any changes that happened in between measurements would not be reflected in the overall load calculation. Indeed many water quality parameters are monitored on monthly, or even quarterly (every 3 months) schedules (Aulenbach, 2008). Depending on the dynamics of the river, this "low-resolution" sampling scheme may omit important data. Figure 2-7 shows a plot of the hourly nitrate load of the Raccoon River at Sac City, Iowa. If this

river were sampled on a monthly basis, many of the peaks and valleys would be omitted and the seasonal load summation would be highly inaccurate.

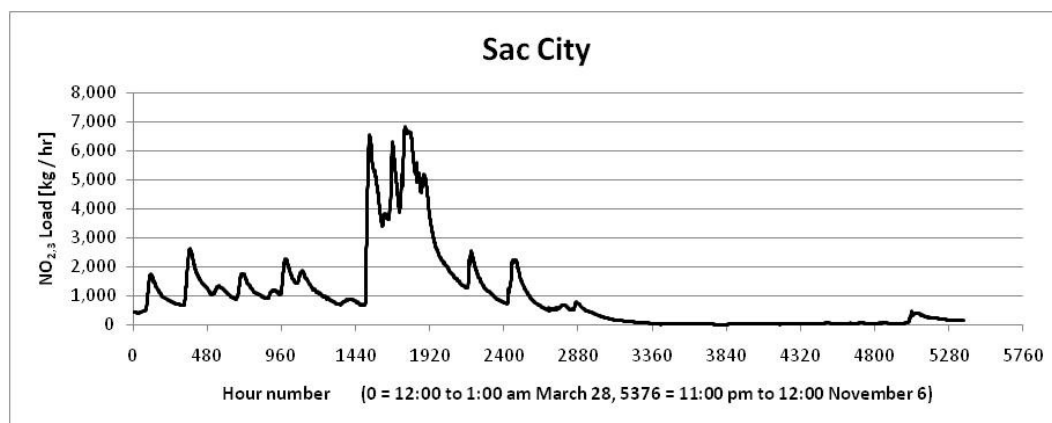


Figure 2-7. High frequency (hourly) nitrate load at Sac City, Iowa. A Hach “Nitratax” probe measured concentration by UV spectroscopy, a USGS gaging station provided discharge data.

A simple numerical experiment was performed to estimate the potential difference in nitrate load summation using different sampling frequencies. High frequency data sets were resampled repeatedly to produce all of the possible load summations under different sampling schemes. The “reference” loads for the stations were first calculated by summing the highest frequency loads available over the entire season. For this experiment these “season loads” were considered the correct values, against which all other load summations would be compared. The resampling schemes for the Raccoon River stations were every two hours, six hours, 12 hours, 24 hours, 7 days, 4 weeks, 8 weeks and 16 weeks; for the Mississippi River stations the schemes were 7 days, 4 weeks, 8 weeks and 16 weeks.

For each scheme there were different possible starting points, each of which produces a different load summation. For example if one were to sample every 6 hours, there would be 6 different times (on the hour) that the sampling could be taken (2 am, 8



am, 2 pm, 8 pm would be one starting point, another would be 3 am, 9 am, 3 pm, and 9 pm and so on). Each “6 hour load interval” would be calculated ( $Q \times C \times 6$  hours), then all 6 hour loads over the season would be summed to produce the season total for that scheme and starting point. Resampling under the same scheme but a different starting point produces a second iteration for that scheme, see also Table 2-1 and Table 2-2. Finally, all iterations for each scheme were compiled and the coefficients of variation were calculated for comparison ( $COV = \text{standard deviation} / \text{arithmetic mean}$ ).

Raw data was acquired for three stations on the Raccoon River in West-Central Iowa. The Raccoon River data sets consisted of discharge and nitrate concentration measurements taken automatically every 15 minutes from March 28, 2008 to November 6, 2008 (hereinafter referred to as the “season”) (nitrate data was collected by a Hach Nitratax probe, discharge data was acquired by typical USGS gaging stations). The raw data contained sporadic zero-points and other probable equipment errors. These points were manually replaced with values linearly interpolated from the bounding non-erroneous points as necessary, and the replacement values were marked as such. The continuous data sets were then reduced to hourly averages of the 15 minute data for two reasons: To reduce overall errors from the previous interpolation step, and to maintain compatibility with the LOADEST software which can only accommodate 24 observations per day.

For large scale comparison, three stations on the Mississippi River were also analyzed (Table 2-3). As high frequency data was not available for these stations “synthetic” high frequency data was used. One output of the operation of the LOADEST model is a set of daily load estimates generated from the regression model. While these daily values would not be considered highly accurate for each specific day they do reflect the discharge based dynamics of the river at each station.

Table 2-1 Number of iterations and samples for each scheme (Raccoon River)

Resampling Scheme	Iterations per Scheme	Samples per Scheme
Hourly (reference scheme)	1	5376
Every 2 hours	2	2688
Every 6 hours	6	896
Every 12 hours	12	448
Every 24 hours	24	224
Every 7 days	168	32
Every 4 weeks	672	8
Every 8 weeks	1344	4
Every 16 weeks	2688	2

Table 2-2 Number of iterations and samples for each scheme (Mississippi River)

Resampling Scheme	Iterations per Scheme	Samples per Scheme
Daily (reference scheme)	1	224
Every 7 days	7	32
Every 4 weeks	28	8
Every 8 weeks	56	4
Every 16 weeks	112	2



Table 2-3 The six gaging stations used for this experiment, and their drainage areas

Gaging Station	River	Drainage Area [mi <sup>2</sup> ]
Sac City	Raccoon	700
Jefferson	Raccoon	1619
Van Meter	Raccoon	3441
Clinton	Mississippi	58,600
Thebes	Mississippi	713,200
Baton Rouge	Mississippi	1,130,000

**CHAPTER 3**  
**RESULTS AND DISCUSSION**  
**NUTRIENT FLUX AND HYPOXIA**

**3.1 Measuring the Size of the 2008 Gulf of Mexico Hypoxic Zone**

The expedition to measure and assess the 2008 Gulf hypoxic zone was successful in delineating the low oxygen plume emanating from the Mississippi and Atchafalaya Rivers. The resulting map of the 2008 hypoxic zone is shown in Figure 3-1. The size in 2008 turned out to be a near record area, approximately 20,700 km<sup>2</sup> (8,000 mi<sup>2</sup>). Although predicted to be a record size of 22,800 km<sup>2</sup> (8,800 mi<sup>2</sup>) due to flood-induced increased freshwater discharge and nutrient inputs, the area was ultimately reduced by the influence of Hurricane Dolly which effectively aerated the West end of the would-be hypoxic plume. (Rabalais, 2008).

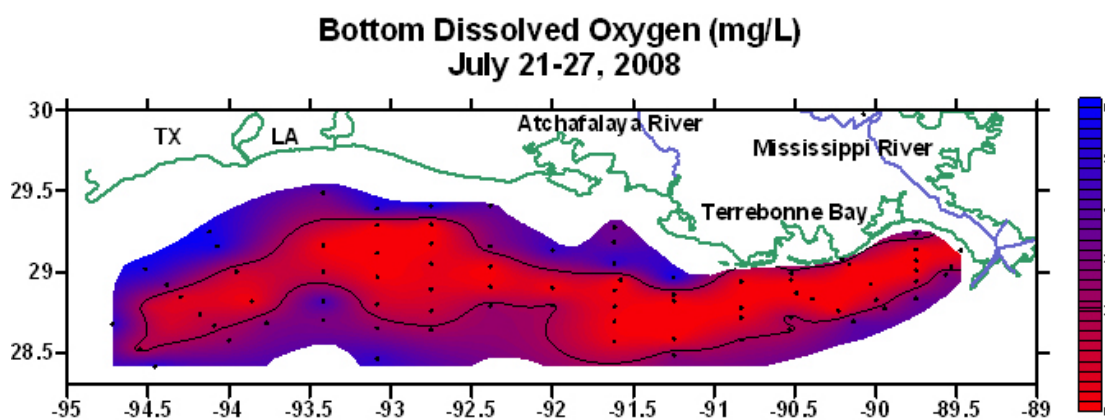


Figure 3-1. The extent of the near-record-size 2008 Gulf of Mexico hypoxic zone (Rabalais, 2008)

During the expedition a number of observations relevant to the state of Gulf hypoxia were made. The area known as the hypoxic zone (or “dead zone”) is not completely without life. The low oxygen plume is confined to the bottom of the water column by a distinct, transient pycnocline (density discontinuity resulting in stratification due to fresh river water on top and saltwater on the bottom). Therefore the water at the surface is not usually hypoxic, this allows non-benthic marine animals to remain alive in the area, as long as they stay near the surface. Benthic animals either flee or die, Figure 3-2 shows a crab swimming at the surface in about 150 foot deep water, this behavior is rare in areas that have sufficient bottom dissolved oxygen. Figure 3-3 shows a bottle nose dolphin jumping out of the water, although a mammal, and therefore unaffected by hypoxia, dolphins typically avoid the hypoxic area as food can become scarce. This dolphin, and all other dolphins observed on the expedition were all at the east edge of the hypoxic area, none were observed in the hypoxic area itself. In the background of Figure 3-3 a difference in water color can be observed. The muddy water in the background is Mississippi River water, contrasted with the darker blue Gulf water in the foreground.

Figure 3-4 shows the only signs of “life” recovered from sediment samples taken from the sea floor in the middle of the hypoxic area, these were a dead polychaete annelid (worm) and a few dead bivalve mollusk shells. Figure 3-5 shows a sediment core sample from the middle of the hypoxic zone. Cores were taken to research long term historical indicators for oxygen depletion, common among them were pockets of black, odiferous, anoxic sediment. Figure 3-6 shows a small squid and fish that were netted at the surface. Also observed at the surface were several baby sharks, jellyfish, and other immature or drifting organisms. No organisms were observed in the hypoxic zone that appeared to be mature non-mammals, despite the fact that the powerful work lights used during the night shift attracted lots of aquatic organisms to the surface near the vessel.



Figure 3-2. This crab was swimming on the surface in 150 foot deep water, an indicator of bottom water dissolved oxygen depletion as crabs are traditionally benthic organisms



Figure 3-3. Bottle nose dolphins swam alongside the research vessel near the east edge of the hypoxic zone, none were observed in the interior of the zone possibly due to reduced abundance of prey.



Figure 3-4. This dead bivalve mollusk and polychaete annelid were the only signs of “life” recovered from sediment samples in the hypoxic zone

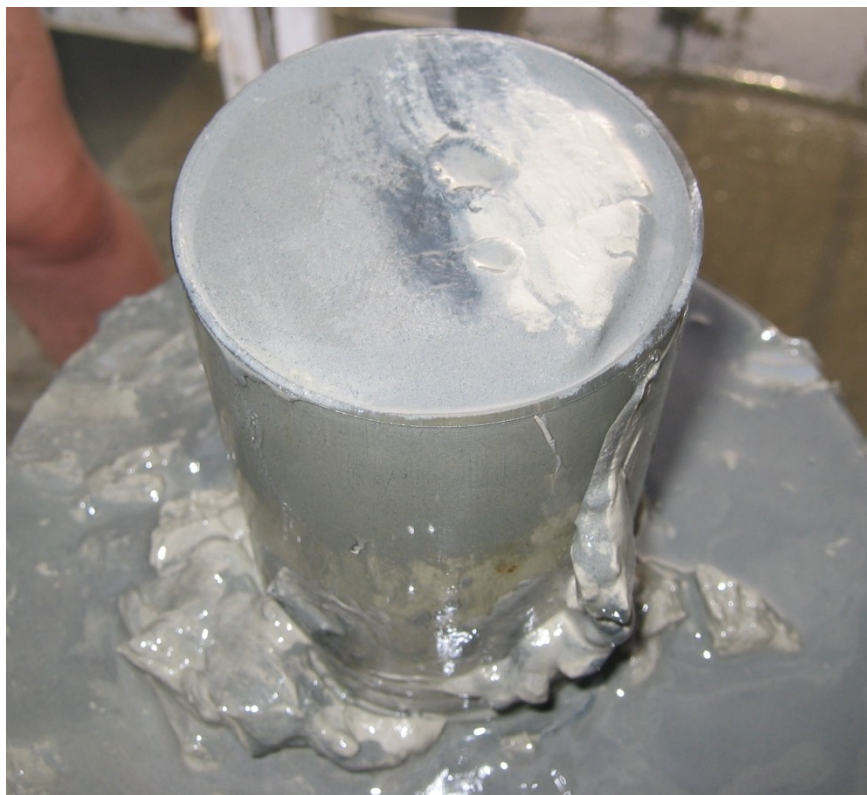


Figure 3-5. The black anoxic streak in this sediment core smelled like sulfide, the cores were used by others to research historical oxygen depletion.





Figure 3-6. This juvenile squid and fish were netted at the surface. The lights used by nighttime work crews attracted all sorts of organisms toward the vessel, yet no mature non-mammals were ever spotted in the hypoxic zone.

### **3.2 2008 Difference in Total Nitrogen Flux** **to the Gulf of Mexico**

The mass of total nitrogen discharged from the MARB to the Gulf of Mexico was significantly higher in water year 2008 than in most prior years. The water-year load was 1.75 million metric tons, whereas the median annual load is 1.4 million metric tons (n=28) (Table 3-1). The 2008 May + June TN sum exceeded the median sum (not including 2008; n=28) by 126,500 metric tons or 34% (95% confidence interval: 111,500 to 159,800 metric tons). Figure 3-7 shows the TN May + June flux for the last 29 years; Figure 3-8 shows the flux difference between water year 2008 and the median, over the course of the year. As much of the Midwestern flooding peaked in mid-late June, the elevated nutrient load arrived at the Gulf approximately one month later.

During May and June 2008, the observed TN flux to the Gulf was 34% greater than the median and the combined MARB fresh water discharge was 42% greater.

Considering the year as a whole, the TN flux was 25% greater than the median annual flux while discharge was 21% greater.

Table 3-1 2008 nitrogen and phosphorus flux by watershed.

Watershed	Area [hax10 <sup>6</sup> ]	% of MARB area	TN Flux [MT]		% of 2008 Gulf TN	TP Flux [MT]		% of 2008 Gulf TP
			Median	2008		Median	2008	
Des Moines -								
Raccoon	3.64	<b>1.13%</b>	52,900	96,300	<b>5.50%</b>	1,930	4,940	<b>6.4%</b>
Iowa - Cedar	3.24	<b>1.00%</b>	67,600	149,000	<b>8.51%</b>	2,600	7,800	<b>10.0%</b>
Wapsipinicon	0.605	<b>0.19%</b>	16,500	33,900	<b>1.93%</b>	481	1,150	<b>1.5%</b>
Turkey	0.400	<b>0.12%</b>	13,900	21,800	<b>1.24%</b>	462	1,250	<b>1.6%</b>
Skunk	1.12	<b>0.35%</b>	22,300	50,000	<b>2.85%</b>	1,330	4,280	<b>5.5%</b>
Illinois	6.93	<b>2.15%</b>	142,000	197,000	<b>11.2%</b>	7,710	17,500	<b>22.5%</b>
<b>TOTAL</b>	<b>15.9</b>	<b>4.94%</b>	<b>315,000</b>	<b>548,000</b>	<b>31.2%</b>	<b>14,500</b>	<b>36,900</b>	<b>47.5%</b>
Entire MARB	323	100%	1,400,000	1,750,000	100%	51,800	77,700	100%



Figure 3-7. May plus June total nitrogen flux from the Mississippi-Atchafalaya River Basin to the Gulf of Mexico, 1980 to 2008. The 2008 flux is shown as the square shape, the median (dashed line) and first and third quartiles (dotted lines) are also shown. Note that this May plus June sum does not include the bulk of the flood load as it likely arrived at these monitoring stations in July.

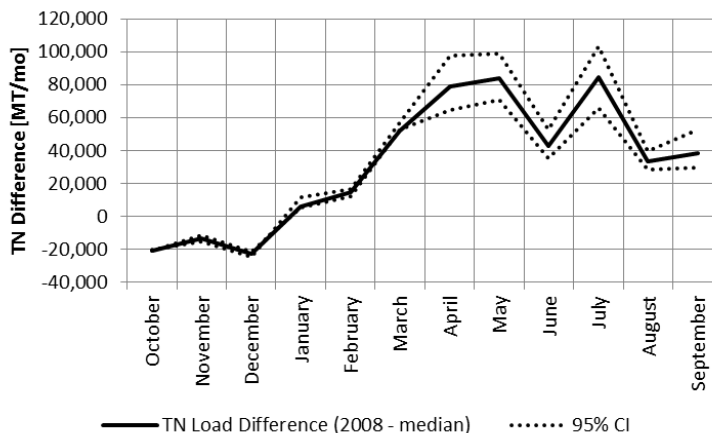


Figure 3-8. The median monthly total nitrogen (n=28) delivered to the Gulf of Mexico from the MARB was subtracted from the 2008 flux to find the difference that occurred each month. Spring flooding that occurred in the Midwest states from March to June is largely responsible for the peaks visible here in April, June, and July, accounting for approximately one month travel time. The dominant hypoxic area prediction model at the time used May and June total nitrogen flux as an input, which would have missed a significant amount of the Midwestern flood flux.

It should also be noted that the year 2008 was chosen because of the recent flooding, but the medians calculated for comparison herein included several other flood years which, depending on the sub-basin, often had significantly higher annual mean discharge rates, especially 1993. Table 3-2 shows the discharge and water yield records for the top 10 discharge years in the period of record for the five main rivers in Iowa, and the upper Mississippi River basin (“UMRB”). The UMRB is represented by the Mississippi River above Grafton, IL minus the Missouri River above Hermann, MO. The medians listed in Table 3-2 are for the period of record including the top discharge years. Figure 3-9 shows a comparative hydrograph for the Mississippi River at Tarbert Landing, MS, which is the last monitoring station before ~30% of the Mississippi flow is diverted to the Atchafalaya River. While 2008 showed very high spring flow, the flooding centered in Iowa didn’t create a particularly anomalous discharge signal by the time it arrived at the Gulf. The late June – early July peak visible in Figure 3-9 represents the bulk of the flood flow as it approached the Gulf of Mexico.



Table 3-2 Top 10 discharge and water yield years for Iowa and the UMRB

Discharge Histories																	
Mississippi R @ Thebes IL minus Missouri R @ Hermann MO (1958-2009)			Iowa River @ Wapello IA (1959-2009)			Skunk R @ Augusta (1915-2009)			DesMoines R @ Keosauqua (1970-2009)			Wapsipinicon R @ DeWitt (1935-2009)			Turkey R @ Garber (1914-2009)		
year	mean CFS	year	mean CFS	year	mean CFS	year	mean CFS	year	mean CFS	year	mean CFS	year	mean CFS	year	mean CFS		
1993	264,200	1993	30550	1993	10200	1993	26920	1993	5461	1993	5461	1993	2905	1993	2905		
2008	221,900	2008	21740	2008	7009	2008	18680	2008	4503	2008	4503	2008	2788	2008	2788		
1973	219,300	1973	17050	1973	6545	1973	16720	1973	3515	1973	3515	1973	2234	1973	2234		
1983	200,900	1983	15700	1974	5417	1983	16100	1983	3060	1973	3060	1973	2092	1973	2092		
1974	186,400	1999	14800	2009	5376	1984	15150	1962	2997	1999	2997	1999	1932	1999	1932		
1986	178,200	1974	13850	1960	4986	2007	12490	1999	2863	1962	2863	1962	1857	1962	1857		
2009	175,060	1984	13220	1998	4906	1974	12410	1982	2807	1951	2807	1951	1680	1951	1680		
1984	170,900	1969	13140	1984	4870	1991	11360	1974	2646	1979	2646	1979	1669	1979	1669		
1982	167,200	2009	12890	1983	4542	1986	11200	1979	2612	1998	2612	1998	1669	1998	1669		
1969	158,100	2007	12700	1962	4519	1998	11140	2007	2584	1982	2584	1982	1598	1982	1598		
Median	130,575		8,913		2,275		8,049		1,597		1,597		987		987		
n =	52		51		95		40		75		75		89		89		

Water Yield Histories																	
Mississippi R @ Thebes IL minus Missouri R @ Hermann MO (DA = 190,700)			Iowa River @ Wapello IA (DA = 12,500 mi <sup>2</sup> )			Skunk R @ Augusta (DA = 4,312 mi <sup>2</sup> )			DesMoines R @ Keosauqua (DA = 14,038 mi <sup>2</sup> )			Wapsipinicon R @ DeWitt (DA = 2,336 mi <sup>2</sup> )			Turkey R @ Garber (DA = 1,545 mi <sup>2</sup> )		
year	CFS mi <sup>-2</sup>	year	CFS mi <sup>-2</sup>	year	CFS mi <sup>-2</sup>	year	CFS mi <sup>-2</sup>	year	CFS mi <sup>-2</sup>	year	CFS mi <sup>-2</sup>	year	CFS mi <sup>-2</sup>	year	CFS mi <sup>-2</sup>		
1993	1.385	1993	2.444	1993	2.365	1993	1.918	1993	2.338	1993	2.338	1993	1.880	1993	1.880		
1973	1.164	2008	1.739	2008	1.625	2008	1.331	2008	1.928	2008	1.928	2008	1.805	2008	1.805		
2008	1.150	1973	1.364	1973	1.518	1973	1.191	1973	1.505	1973	1.505	1973	1.446	1973	1.446		
1983	1.053	1983	1.256	1974	1.256	1983	1.147	1983	1.310	1973	1.310	1973	1.354	1973	1.354		
1974	0.977	1999	1.184	2009	1.247	1984	1.079	1962	1.283	1999	1.283	1999	1.250	1999	1.250		
1984	0.934	1974	1.108	1960	1.156	2007	0.890	1999	1.226	1962	1.226	1962	1.202	1962	1.202		
1986	0.918	1984	1.058	1998	1.138	1974	0.884	1982	1.202	1951	1.202	1951	1.087	1951	1.087		
1999	0.896	1969	1.051	1984	1.129	1991	0.809	1974	1.133	1979	1.133	1979	1.080	1979	1.080		
1951	0.877	2009	1.031	1983	1.053	1986	0.798	1979	1.118	1998	1.118	1998	1.080	1998	1.080		
1998	0.829	2007	1.016	1962	1.048	1998	0.794	2007	1.106	1982	1.106	1982	1.034	1982	1.034		
Median	0.685		0.713		0.528		0.573		0.684		0.684		0.639		0.639		

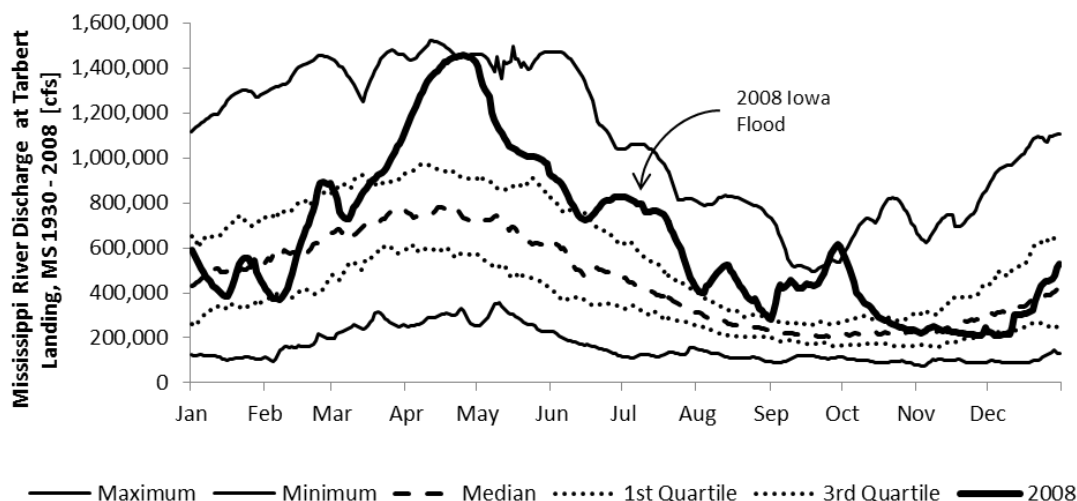


Figure 3-9. The Mississippi River hydrograph for Tarbert Landing, MS (the southernmost gaging station before approximately 30% of the flow is re-directed to the Atchafalaya River). The large anomalous peak in late April is primarily from heavy spring rains in the Ohio River basin, the lesser peak at the beginning of July is the floodwater from the June floods centered in Iowa. As the hypoxia prediction model uses the May and June flux near this station, a large portion of the Midwestern flood would not have been included in the predictions.

### **3.3 Nutrient Flux Due to Flooding** **in Agricultural Watersheds**

Table 3-1 lists the estimated nitrogen and phosphorus fluxes from five watersheds in Iowa and the Illinois River, as well as the MARB as a whole. These six sub-watersheds exported nearly one third of the nitrogen, and half of the phosphorus that entered the Gulf of Mexico in 2008, yet represent only 5% of the Mississippi / Atchafalaya river basin. The portion of land area in each basin covered by corn fields ranged from 32.2% to 43.4%, and 9% for the entire MARB. The median values listed in Table 3-1 include all years of record except 2008.

### **3.4 Potential Difference in Area of Hypoxia due to Additional Nitrogen**

The total difference in hypoxic area predicted by the 1-D dissolved oxygen sag model was 2,370 square kilometers or 915 square miles (95% confidence intervals: 2,290 to 2,490 km<sup>2</sup> or 884 to 960 mi<sup>2</sup>). This area corresponds to a plume length of ~60 kilometers. These values represent the theoretical expansion of the hypoxic plume due only to the increase in TN loading delivered in May and June 2008.

A simple metric was established by which to qualitatively assess the impact of each watershed on the hypoxic area. The theoretical area of hypoxia attributed to each watershed was estimated by proportioning the total predicted 2008 hypoxic zone size by the fraction of May + June TN load at the gulf represented by the April + May TN load at the base of each Iowa watershed (accounting for travel time of approximately one month). Figure 3-10 proportions the “hypoxic yield” by watershed area, and Figure 3-11 proportions by the area planted in corn in each watershed during 2008. The actual values should be used for comparison only as there are clearly more sources of in-stream nitrogen than just corn fields, however as corn fields are a major nitrogen contributor, knowledge is potentially gained from normalizing nutrient flux by corn area in neighboring basins. In-river loss of TN is assumed to be relatively minor (<10%) in the mid to lower Mississippi River as the literature has demonstrated (Alexander, 2008).

### **3.5 Nutrient Flux Scaling Over a Range of Drainage Areas**

The Mississippi River basin is a vast area with diverse land usage. While it encompasses all of the area known as the US ‘corn belt’, it also drains large areas that are not devoted to row-crop production. As one objective of this research is to document the origin and behavior of flood scale nutrient flux, 11 watersheds were assessed which range in size from small local rivers to the entire MARB. Figure 3-12 through Figure 3-17 compare the flux that occurred during the three highest flow years in each watershed to

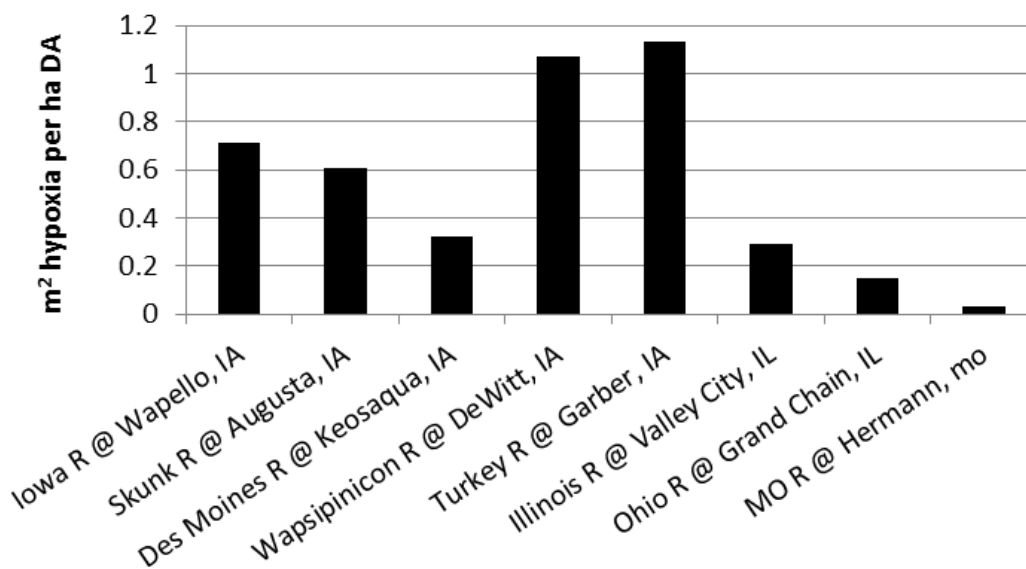


Figure 3-10. Assuming that the 2008 April + May TN flux from each watershed represents a portion of the May + June TN flux at the Gulf outlets (roughly accounting for travel time), then that same proportion could be applied to the total predicted hypoxic area. Dividing the predicted area of hypoxia that each watershed is represents by the drainage area of the watershed gives a comparative metric of “area of hypoxia per area of watershed.

the corresponding local median flux. In all but one case, the slope of a least-squares linear regression is notably less for the flood scale flux than the median, the magnitude of the difference depends upon the characteristics of each nutrient and watershed.

While the logarithmically plotted data in Figure 3-12 through Figure 3-17 were fitted with linear regressions for simplicity, the important patterns are not necessarily linear (despite the relatively high  $R^2$  values). For example the graph of nitrate + nitrite vs. DA (Figure 3-13) clearly shows a pattern of attenuating yield as the drainage area increases. This is logical as the smaller watersheds chosen for this analysis are heavily planted in row-crops, particularly corn, and the larger ones are increasingly heterogeneous in land use.

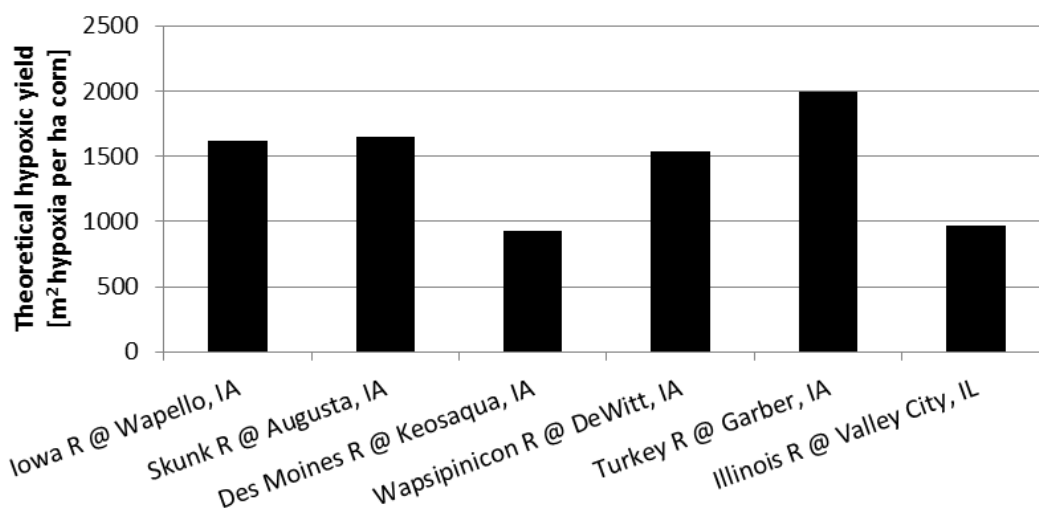


Figure 3-11. Corn area hypoxic yield; similar to Figure 3-10 the predicted hypoxic area was proportioned by individual watershed TN flux. In this case the area in each watershed planted in corn during 2008 was used. Of course not all nitrogen flux came specifically from corn fields, however this gives a more accurate qualitative yield depiction than Figure 3-10 because it accounts for the varying corn acreage

### **3.6 Agricultural Costs of Flood Scale Nutrient Export**

Looking only at fertilizer inputs and stream borne outputs, various fractions can be gleaned from the literature comparing the amount of chemical nitrogen fertilizer applied to corn fields with the amount of nitrogen flux in adjacent local streams and rivers. Other researchers (Libra, et al., 2004; Goolsby, Battaglin and Thurman, 1993; Buzicky et al., 1983) have found average nitrogen loss-to-stream rates to be 18% to 35% of application rates during average to dry years. Buzicky et al. (1983) assessed experimental corn fields specifically and found  $38 \text{ kg N ha}^{-1} \text{ yr}^{-1}$  in streams when application rates were  $202 \text{ kg N ha}^{-1} \text{ yr}^{-1}$  (18.8% loss). From the IDNR mass balances conducted on nitrogen in Iowa soils it can be estimated that stream loads were 20.1% of chemical nitrogen fertilizer applications, this result was calculated during a particularly dry period. Data analysis for this research found similar mean loss fractions of 16% to 22% (during median flow years) depending on application rate and data source.

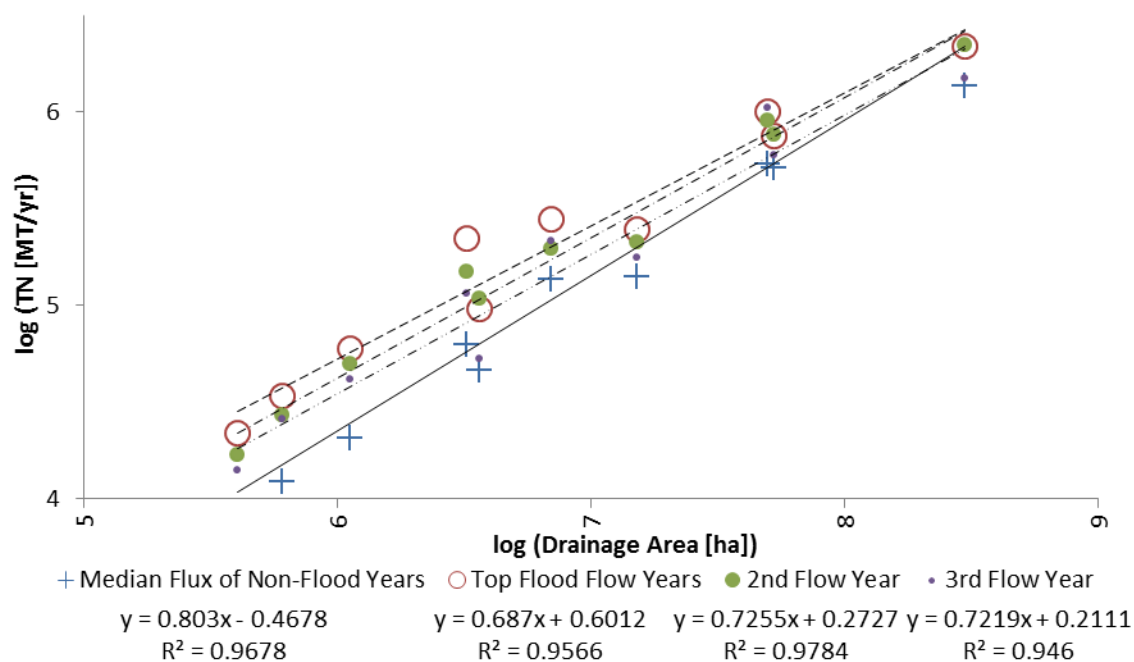


Figure 3-12. Total nitrogen yield scaling. The solid line is a least squares regression of the median flux for non-flood flow years. The dashed line is the flux for the highest flow years (which could be different for each watershed). The dashed, one-dot line is the flux for the second highest flow years, and the dashed, two-dot line is the flux for the third highest flow years. The median values display a more linear relationship than the flood years and all log-log slopes are less than one, the flood year slopes are approximately 11.4% less than the median slope. This indicates that the rate of flux attenuation over increasing drainage area increases for the flood years, and that the flux-increasing effect of flooding is most prominent in the middle range of drainage areas.

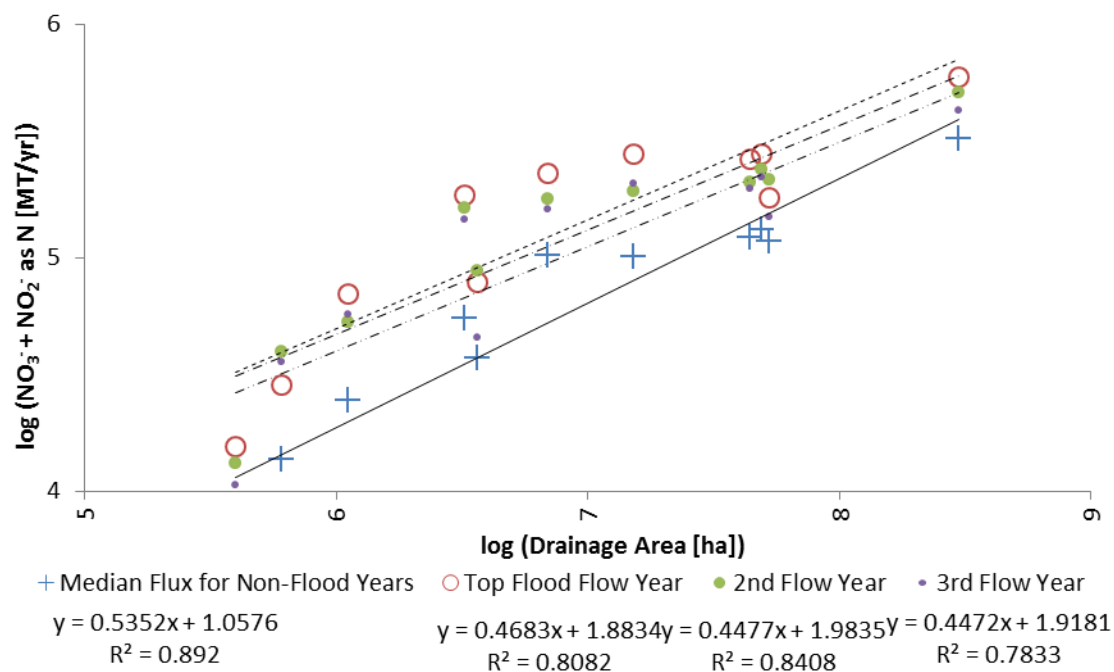


Figure 3-13. Nitrate + nitrite yield scaling. The solid line is a least squares regression of the median flux for non-flood flow years. The dashed line is the flux for the highest flow years (which could be different for each watershed). The dashed, one-dot line is the flux for the second highest flow years, and the dashed, two-dot line is the flux for the third highest flow years. The median values display a more linear relationship than the flood years and all log-log slopes are less than one, the flood year slopes are approximately 15% less than the median slope. This indicates that the rate of flux attenuation over increasing drainage area increases for the flood years, and that the flux-increasing effect of flooding is most prominent in the middle range of drainage areas.

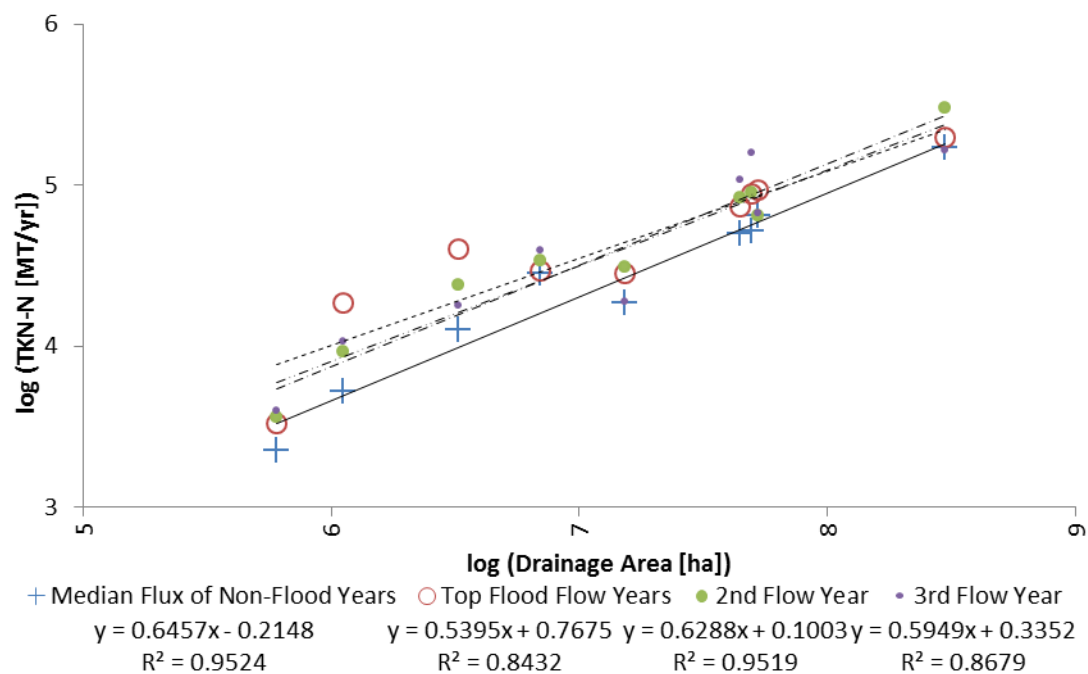


Figure 3-14. Total Kjeldahl nitrogen yield scaling. The solid line is a least squares regression of the median flux for non-flood flow years. The dashed line is the flux for the highest flow years (which could be different for each watershed). The dashed, one-dot line is the flux for the second highest flow years, and the dashed, two-dot line is the flux for the third highest flow years. The median values display a more linear relationship than the flood years and all log-log slopes are less than one, the flood year slopes are approximately 9% less than the median slope. This indicates that the rate of flux attenuation over increasing drainage area increases for the flood years, and that the flux-increasing effect of flooding is most prominent in the middle range of drainage areas.



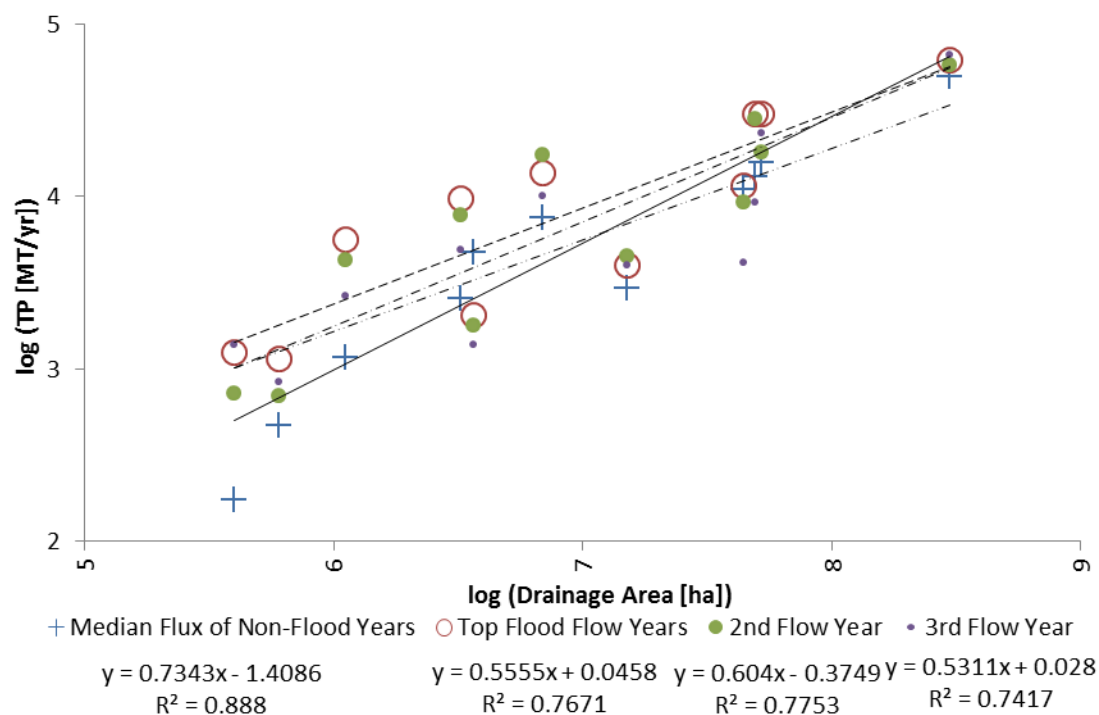


Figure 3-15. Total unfiltered phosphorus yield scaling. The solid line is a least squares regression of the median flux for non-flood flow years. The dashed line is the flux for the highest flow years (which could be different for each watershed). The dashed, one-dot line is the flux for the second highest flow years, and the dashed, two-dot line is the flux for the third highest flow years. The median values display a more linear relationship than the flood years and all log-log slopes are less than one, the flood year slopes are approximately 37% less than the median slope. This indicates that the rate of flux attenuation over increasing drainage area increases for the flood years, and that the flux-increasing effect of flooding is most prominent in the middle range of drainage areas.

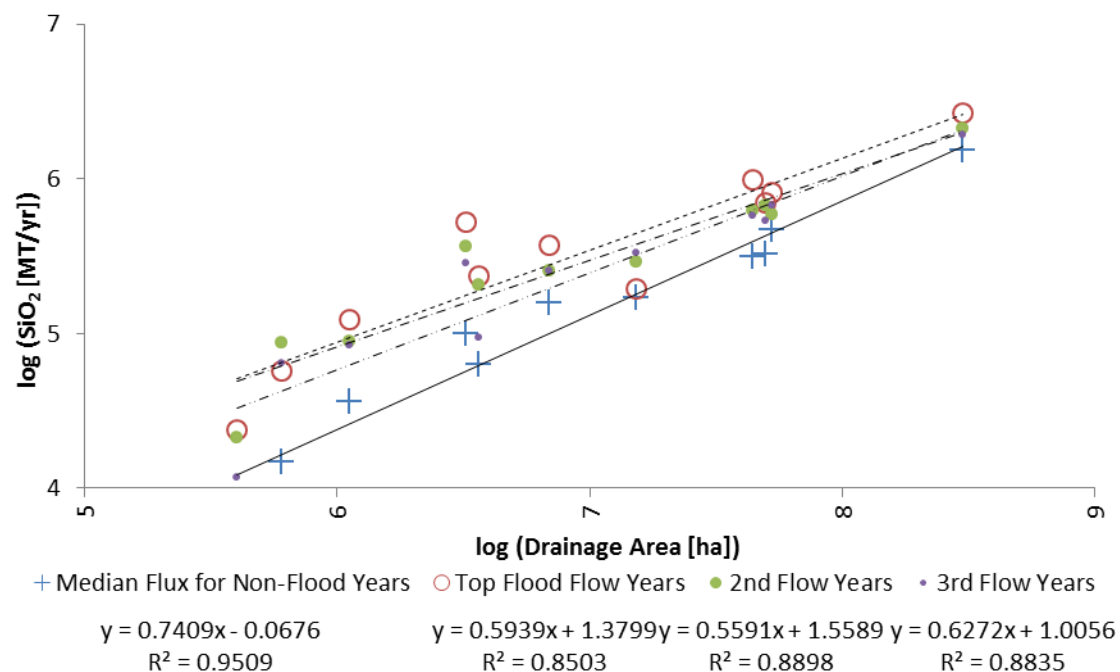


Figure 3-16. Dissolved silica ( $\text{SiO}_2$ ) yield scaling. The solid line is a least squares regression of the median flux for non-flood flow years. The dashed line is the flux for the highest flow years (which could be different for each watershed). The dashed, one-dot line is the flux for the second highest flow years, and the dashed, two-dot line is the flux for the third highest flow years. The median values display a more linear relationship than the flood years and all log-log slopes are less than one, the flood year slopes are approximately 20% less than the median slope. This indicates that the rate of flux attenuation over increasing drainage area increases for the flood years, and that the flux-increasing effect of flooding is most prominent in the middle range of drainage areas.

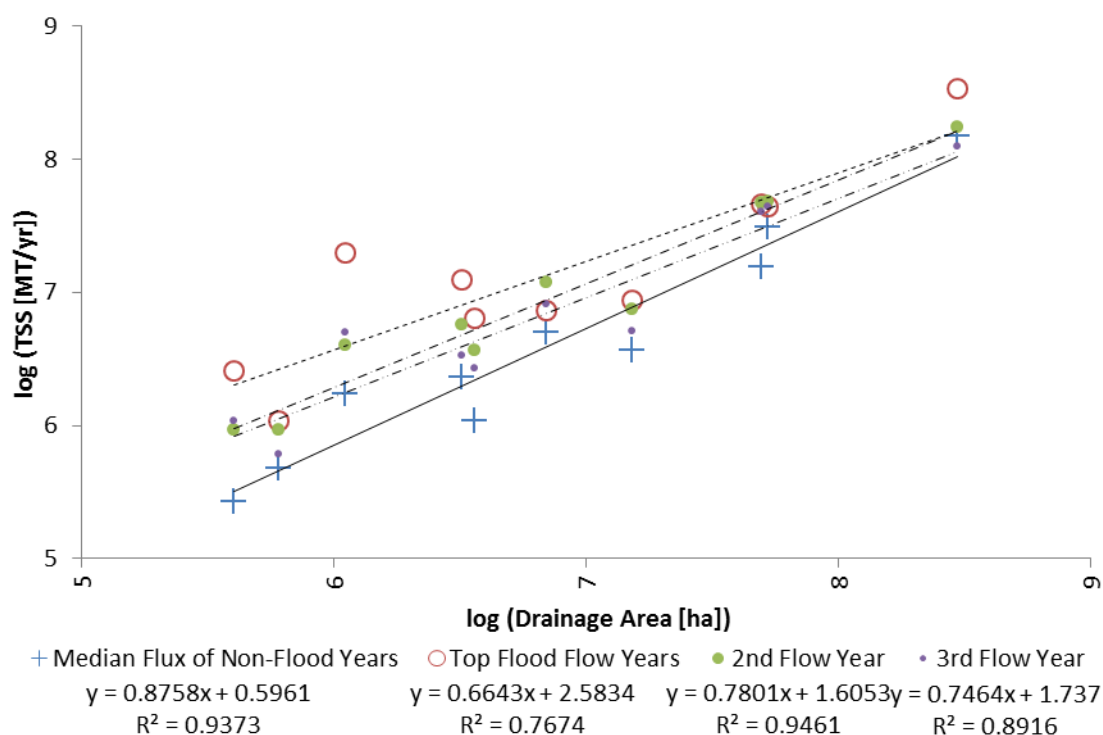


Figure 3-17. Total suspended solids yield scaling. The solid line is a least squares regression of the median flux for non-flood flow years. The dashed line is the flux for the highest flow years (which could be different for each watershed). The dashed, one-dot line is the flux for the second highest flow years, and the dashed, two-dot line is the flux for the third highest flow years. The median values, in general, display a more linear relationship than the flood years and all log-log slopes are less than one, the flood year slopes are approximately 16.6% less than the median slope. This indicates that the rate of flux attenuation over increasing drainage area increases for the flood years, and that the flux-increasing effect of flooding is most prominent in the middle range of drainage areas.

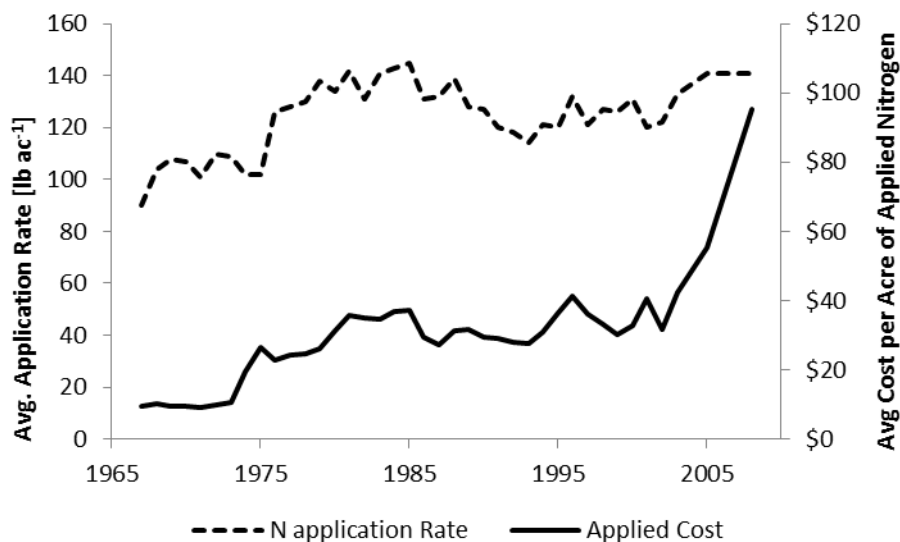


Figure 3-18. Both the application rate and cost of nitrogen fertilizer has risen sharply since the 'green revolution'. This graph of Iowa data shows the combination as the average April cost of applied nitrogen fertilizer per acre (average of all common forms) (USDA-NASS, 2010).

During 2008 when the number of corn acres planted was particularly high, extraordinarily high precipitation occurred just after the typical fertilizing season, and chemical fertilizer usage rates were high (the prices for those fertilizers were also at record highs, see Figure 3-18) an extraordinarily large fraction of nitrogen ran off of Iowa corn fields. The five assessed watersheds representing 63% of Iowa lost 351,000 metric tons of nitrogen via streams (95% CI: 333,000 to 372,620); scaling up to all of Iowa by area gives an estimated 560,000 metric tons of nitrogen lost via streams (95% CI: 531,000 to 593,000). Figure 3-19 shows the combined flux from 5 Iowa watersheds and the median flux, Figure 3-20 shows the 2008 TN flux from the 5 watersheds compared to their individual median fluxes.

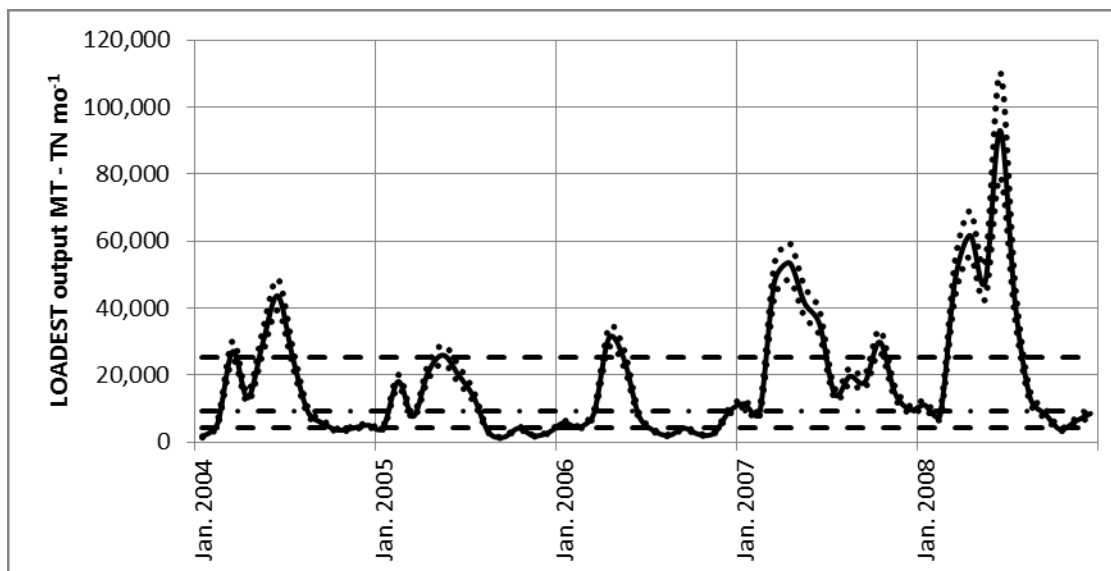


Figure 3-19. LOADEST output of total nitrogen flux for 5 watersheds comprising 63% of Iowa. 95% confidence intervals are shown (dotted lines), as are the 5 year median and first and third quartiles. The median monthly flux was 9,418 MT N, whereas the June 2008 flux was 93,000 MT N (95% CI: 79,000 to 110,000).

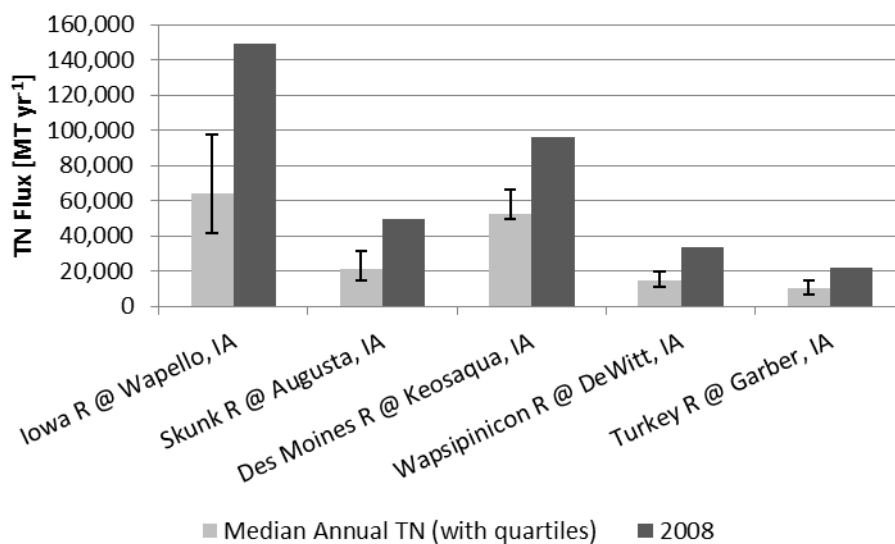


Figure 3-20. Total nitrogen flux for each of the five biggest watersheds in Iowa. The 2008 flux was significantly greater than the 3<sup>rd</sup> quartile flux in all cases.

Based on an application rate of 141 lb N per corn acre (USDA-NASS, 2005; the most recent published data from the USDA) and an average of \$0.68 per pound of applied nitrogen (USDA-ERS, 2008), applying chemical nitrogen fertilizer to corn fields cost Iowa farmers approximately \$95.20 per acre (phosphorus cost an average of \$2.27 per pound applied), see Figure 3-18. In 2008, there were 13,700,000 acres planted in corn and 99% received some form of nitrogen fertilizer (USDA-NASS, 2010). By extension Iowa farmers applied approximately 872,000 metric tons of nitrogen at an approximate cost of \$1.3 billion. These figures do not include the application of manure, waste-water treatment plant solids, industrial solids, etc., only commercial chemical nitrogen.

Using a simplified comparison of fertilizer inputs to stream-borne outputs, the mass of nitrogen flux from the five Iowa watersheds in 2008 was 64% of the mass of nitrogen applied to corn fields alone in the same area (560,000 MT estimated stream flux / 872,000 MT fertilizer). This represents a loss of approximately \$525 million for those watersheds (95% CI: \$498 million to \$558 million) or \$834 million for the entire state (scaled up by multiplying by 1/0.63). For comparison, the “scaled up” median nitrogen flux from Iowa (270,300 metric tons) divided by the 2005 application rate is 31%, still a bit higher than typical loss rates, but half as much as that which occurred in 2008.

Figure 3-21 shows the approximate value of nitrogen exported from 5 watersheds in Iowa while Figure 3-22 shows the actual nitrogen yield by whole watershed area and Figure 3-23 shows the yield specific to the corn area in each watershed. Again, the source of estimated in-stream flux is not just corn, however farmers growing corn will have to pay for fertilizer to replace the lost nitrogen in order to maintain yields, therefore it is worth visualizing a metric for the long term cost of nutrient replacement.

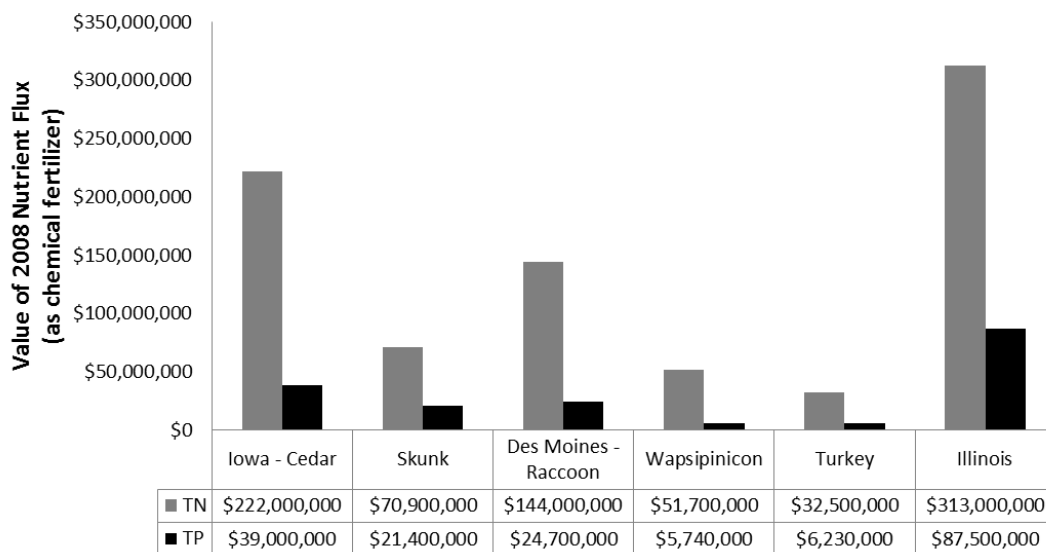


Figure 3-21. Total value of nitrogen and phosphorus exported by watershed. At least 16% of this nitrogen had natural, non-fertilizer origins, nonetheless a significant fraction of applied fertilizer likely ran off over the course of the year.

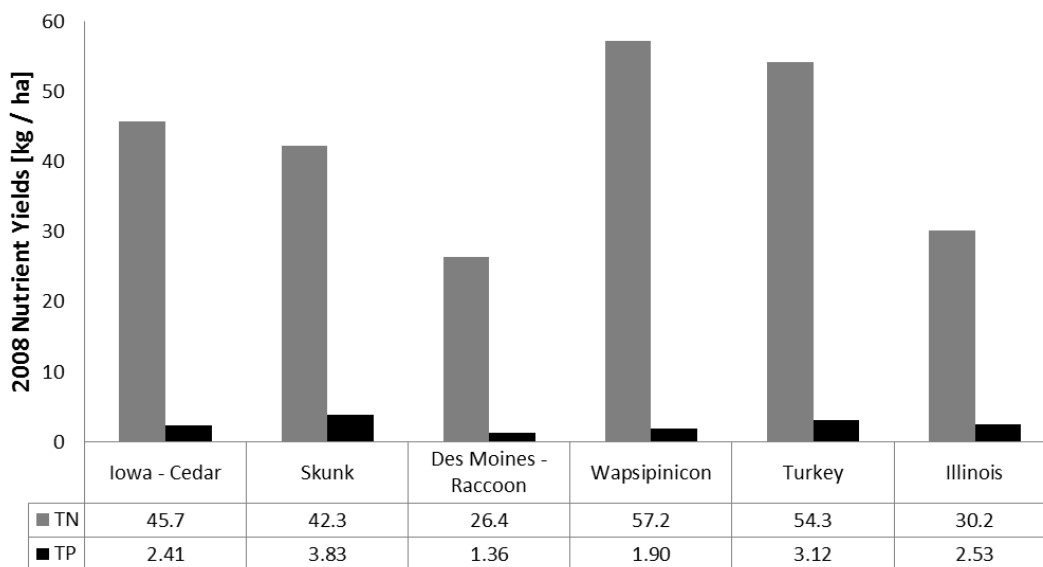


Figure 3-22. Total nitrogen and phosphorus yields from whole Iowa watersheds during 2008, this is the water-borne flux divided by each drainage area.

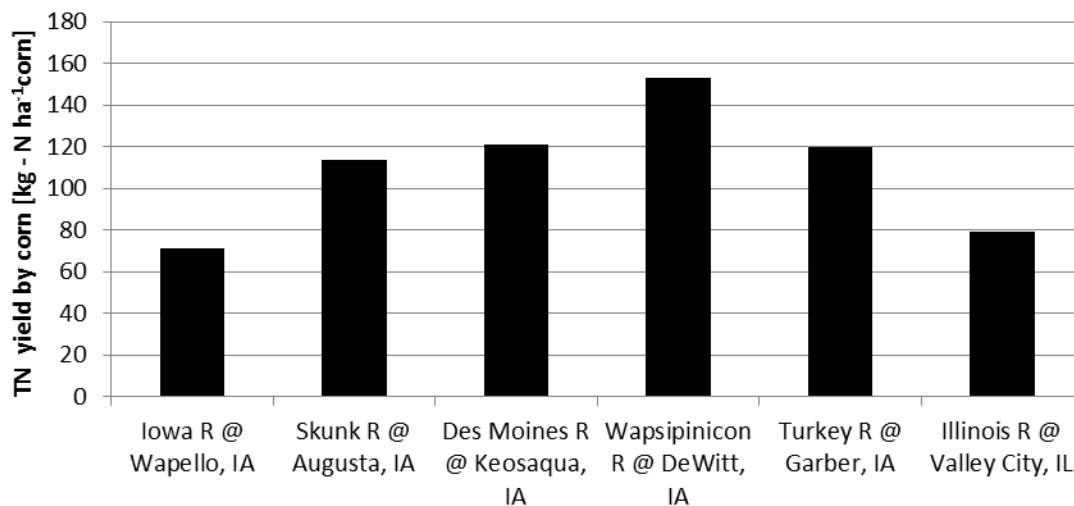


Figure 3-23. Total nitrogen yield from the corn area in each watershed. This is the flux from the entire drainage area divided by only the area planted in corn in each watershed. The nitrogen likely came from many sources, however corn agriculture is the largest non-point source.



**CHAPTER 4**  
**RESULTS AND DISCUSSION**  
**SAMPLING FREQUENCY**

**4.1 Optimal Sampling Frequency for**  
**Accurate Load Estimation**

In order to maintain confidence in nutrient load estimates, the water quality samples that the estimates – which are essentially numerical summations of periodic sampling results – are based on must be made at high “enough” frequencies. This analysis aims to provide a framework for answering the question “How high is high enough?”.

The Raccoon River nitrate load data sets used were based on the discharge and concentration data shown in Figure 4-1, Figure 4-2, and Figure 4-3. An interesting observation can be made in these figures regarding the changing correlation of concentration “C” and discharge “Q”. As a storm event begins and Q first increases, C drops; then C increases as the storm continues. As the storm discharge recedes, C recedes slowly. The relationship between the two is first negative, then positive, then loosely positive. This hysteresis can also be seen in Figure 4-4, Figure 4-5, and Figure 4-6, which are logarithmic plots of Q versus C. At high discharge concentration tends to drop, and the effect increases as drainage area increases (Sac City < Jefferson < Van Meter). This inconsistent correlation is why load models based on discharge tend to produce errors, especially during anomalous events such as flooding.

**4.2 Statistical Analysis of Resampled**  
**High Frequency Data Sets**

Upon resampling the high frequency data sets at different frequencies, each station displayed varying degrees of inaccuracy with increasing sampling interval. The mean of the resulting load values computed for each iteration was identical each time,

this is mathematically predictable if the iterations are performed correctly. The standard deviation of the iterative sets increased with each increasing resampling scheme. Figure 4-7 displays this concept. In order to compare the variation quantitatively, coefficients of variation were computed (standard deviation normalized by the mean).

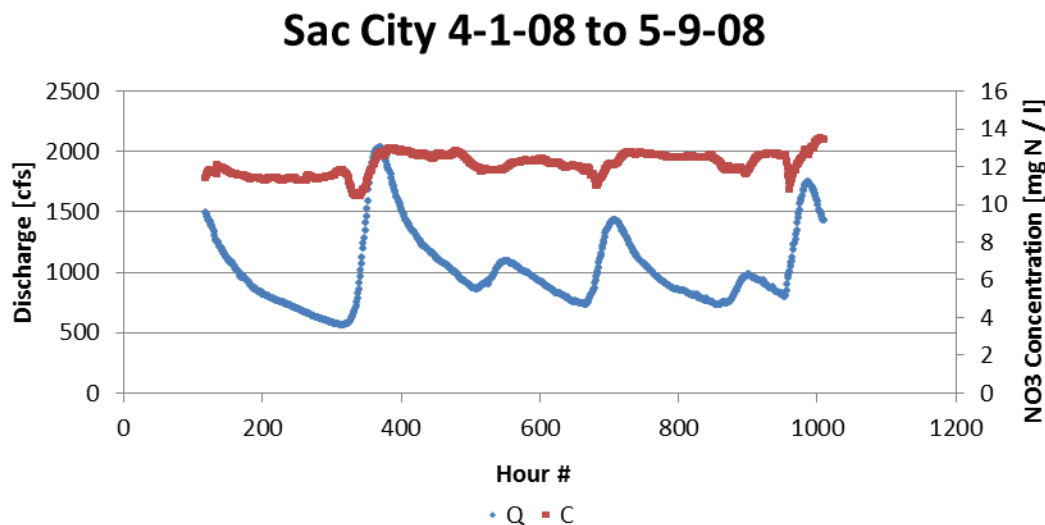


Figure 4-1. Hourly discharge and nitrate concentration on the Raccoon River at Sac City.

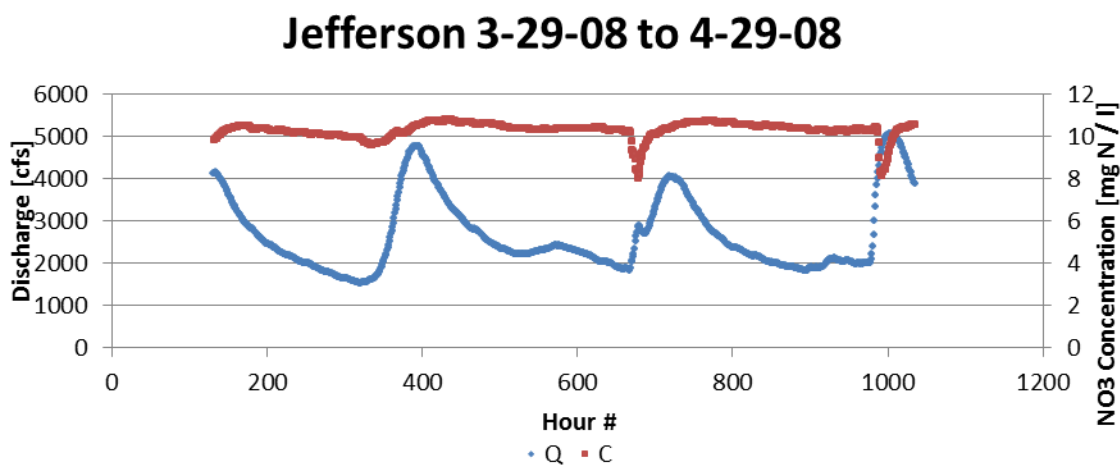


Figure 4-2. Hourly discharge and nitrate concentration on the Raccoon River at Jefferson.

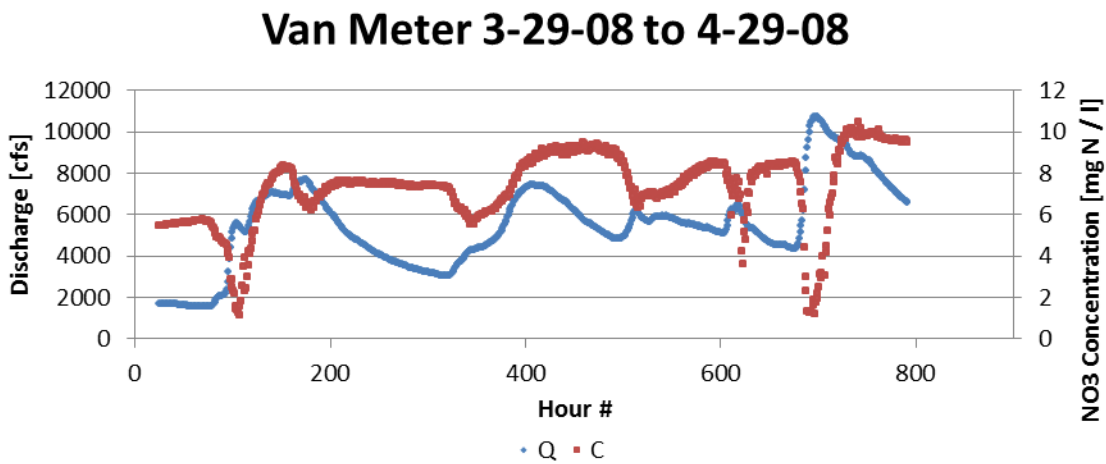


Figure 4-3. Hourly discharge and nitrate concentration on the Raccoon River at Van Meter

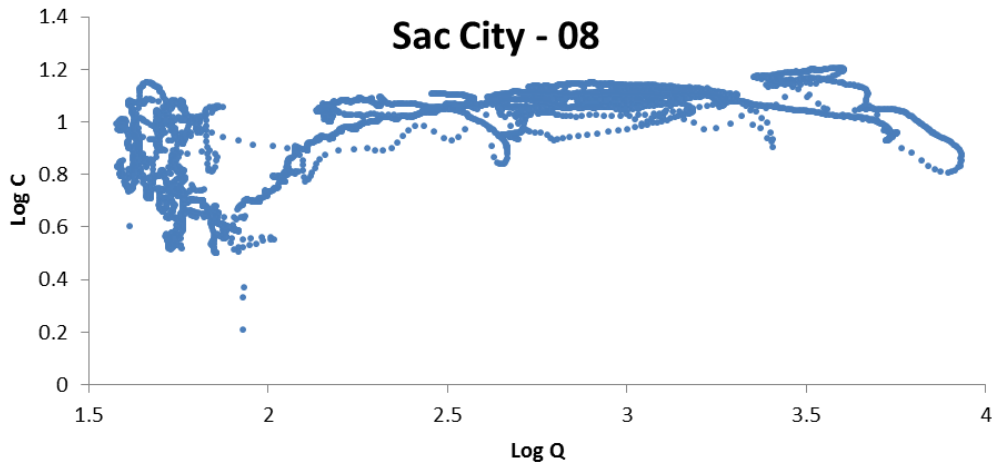


Figure 4-4. Logarithmic comparison of discharge to concentration for the Raccoon River at Sac City.

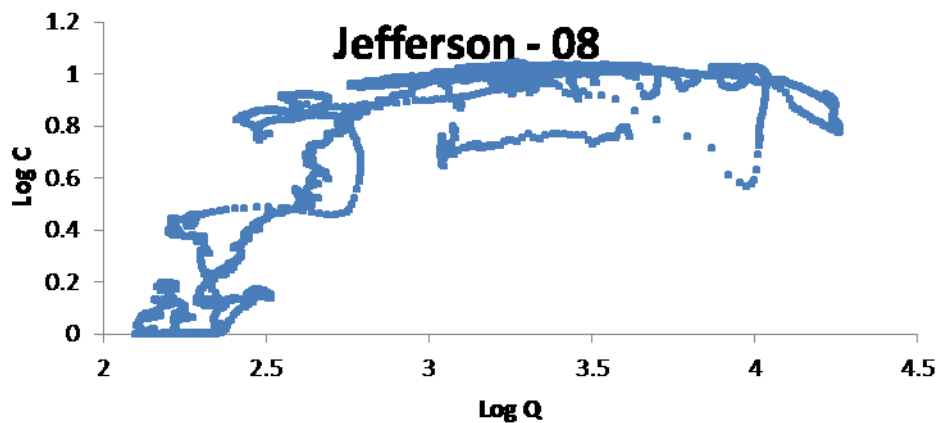


Figure 4-5. Logarithmic comparison of discharge to concentration for the Raccoon River at Jefferson.

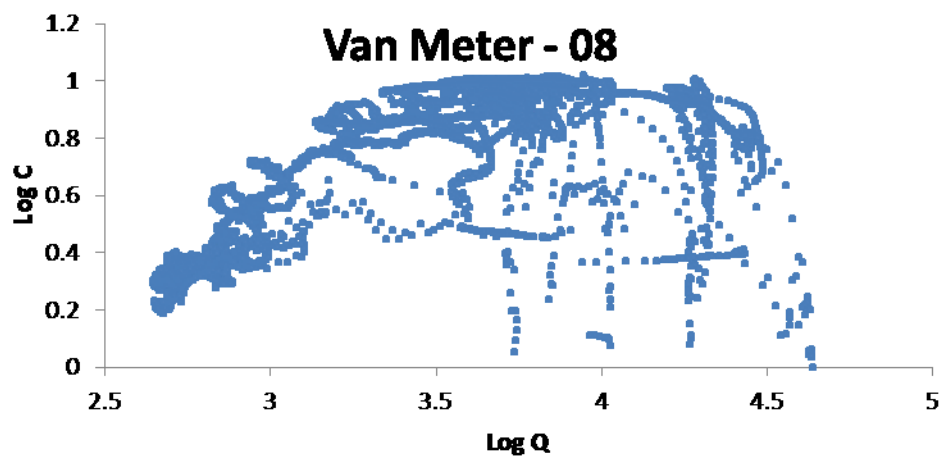


Figure 4-6. Logarithmic comparison of discharge to concentration for the Raccoon River at Van Meter.

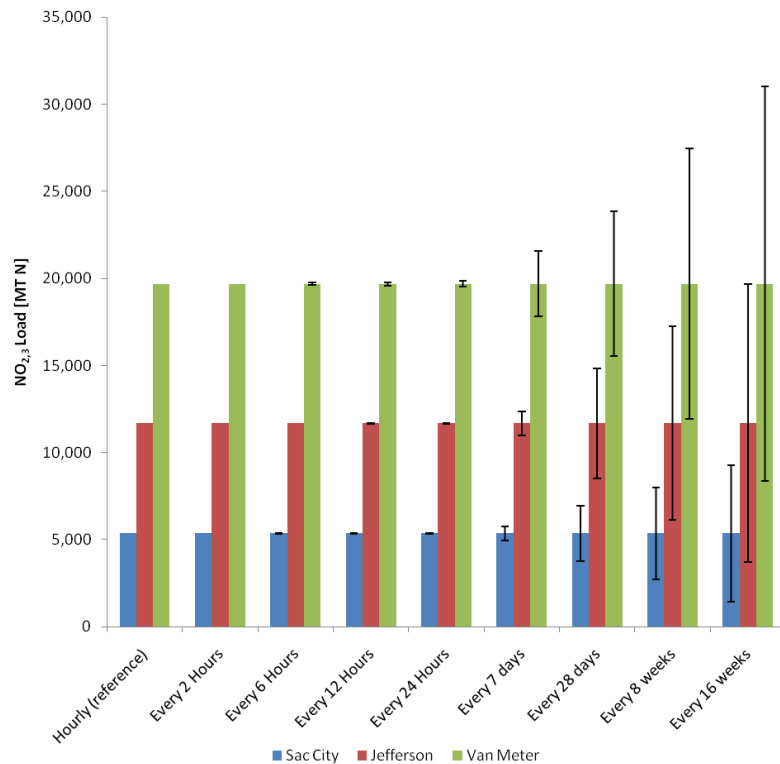


Figure 4-7. Comparative column chart showing increasing error as sampling interval is increased. The columns themselves are the means of each iteration set

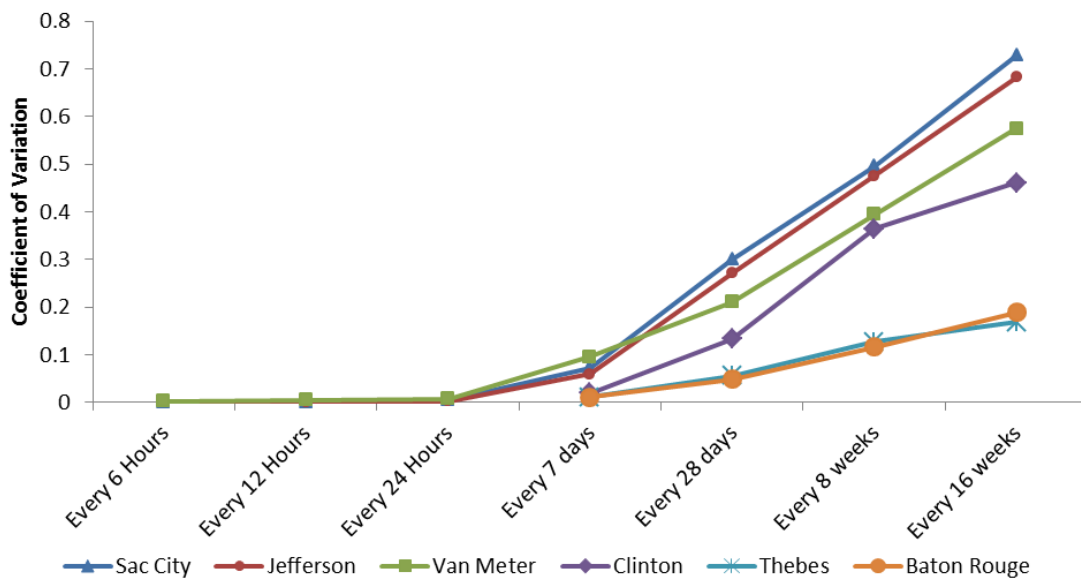


Figure 4-8. The coefficients of variation for all resampling sets. Note that as the sampling frequency increases, the coefficient of variation increases, but it increases the most for the smallest drainage area and the least for the largest drainage areas.

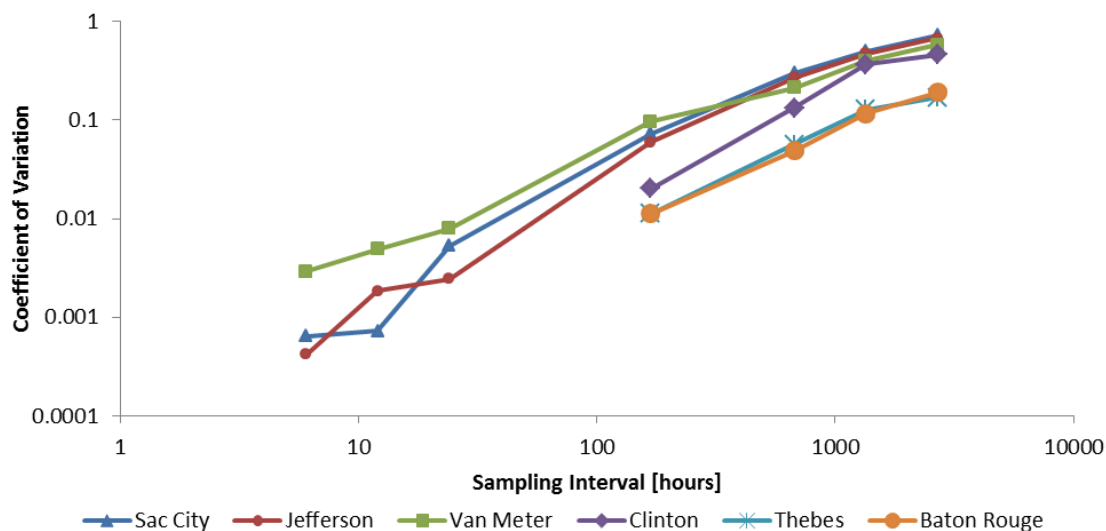


Figure 4-9. Log-Log plot of Figure 4-8, this version better shows the dynamics at the lowest end of the sampling frequency spectrum

Table 4-1 Data from the sampling frequency experiment (Raccoon River)

Summing Scheme	n =	COV		
		Sac City	Jefferson	Van Meter
Hourly (reference scheme)	1	N/A	N/A	N/A
Every 2 hours	2	N/A	N/A	N/A
Every 6 hours	6	0.00042	0.00064	0.00291
Every 12 hours	12	0.00184	0.000724	0.00488
Every 24 hours	24	0.00244	0.00530	0.00787
Every 7 days	168	0.0595	0.0726	0.0960
Every 4 weeks	672	0.271	0.300	0.211
Every 8 weeks	1344	0.475	0.496	0.395
Every 16 weeks	2688	0.682	0.729	0.575

Table 4-2 Data from the sampling frequency experiment (Mississippi River)

Summing Scheme	n =	COV		
		Clinton	Thebes	Baton Rouge
Daily (reference scheme)	1	N/A	N/A	N/A
Every 7 days	7	0.0203	0.0111	0.0112
Every 4 weeks	28	0.133	0.0563	0.0488
Every 8 weeks	56	0.365	0.127	0.116
Every 16 weeks	112	0.461	0.168	0.190

Table 4-1 and Table 4-2 show the actual results of the experiment, which were used to create Figure 4-8 and Figure 4-9. Another way to visualize the increasing error with increasing sampling interval is to plot all seasonal load values computed for each iteration in a way that compares them with the “correct” seasonal load value. This comparison is made in Figure 4-10 through Figure 4-15, note that the scales in each figure are different to show the increasing minima, maxima, and overall lack of accuracy.

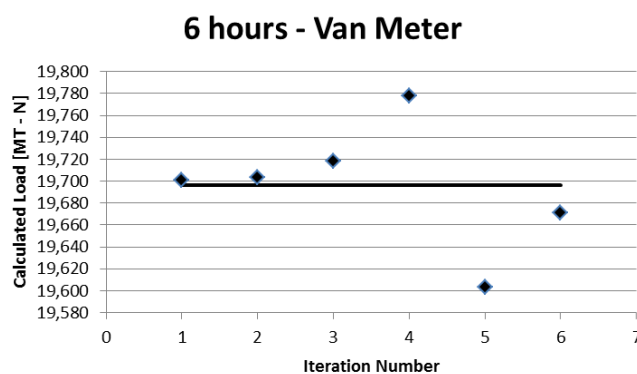


Figure 4-10. Seasonal loads generated by sampling every 6 hours. The hourly reference load is represented by the line at 19,700 metric tons - N

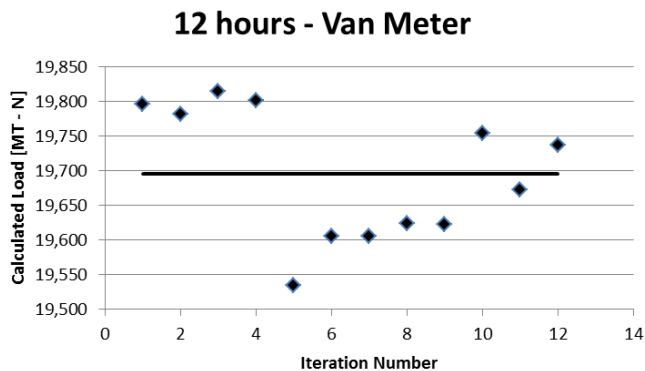


Figure 4-11. Seasonal loads generated by sampling every 12 hours. The hourly reference load is represented by the line at 19,700 metric tons - N

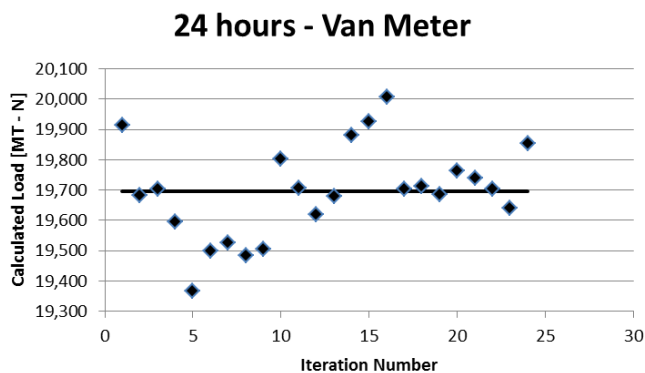


Figure 4-12. Seasonal loads generated by sampling every 24 hours. The hourly reference load is represented by the line at 19,700 metric tons - N

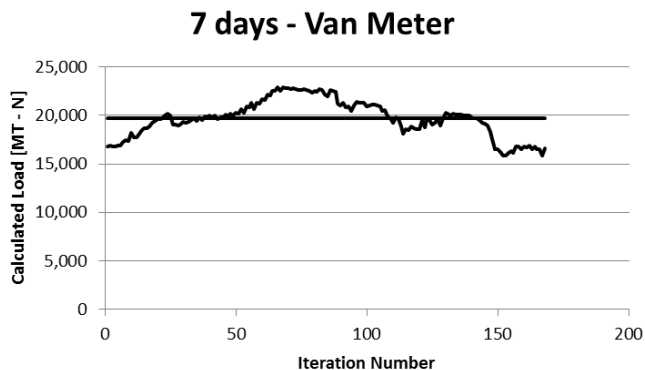


Figure 4-13. Seasonal loads generated by sampling every 7 days. The hourly reference load is represented by the line at 19,700 metric tons - N



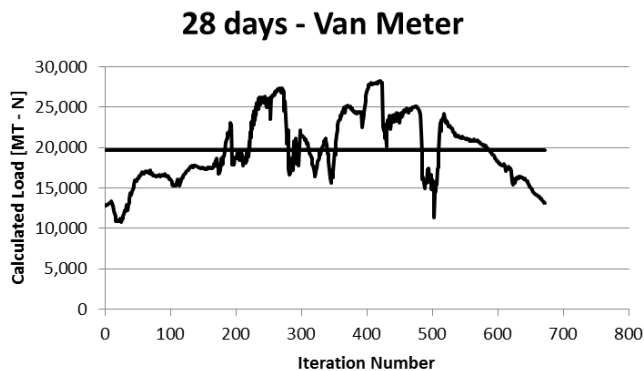


Figure 4-14. Seasonal loads generated by sampling every 28 days. The hourly reference load is represented by the line at 19,700 metric tons - N

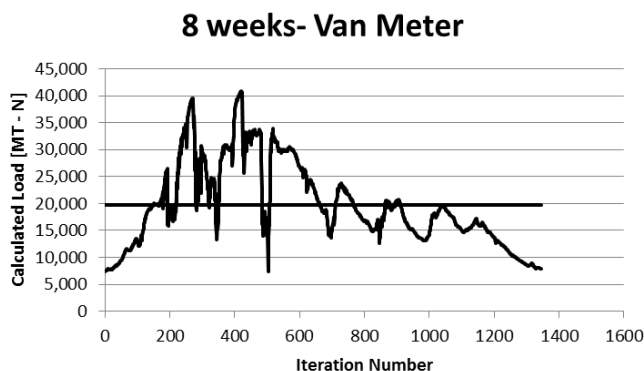


Figure 4-15. Seasonal loads generated by sampling every 8 weeks. The hourly reference load is represented by the line at 19,700 metric tons – N

The optimal sampling frequency clearly depends on the river, the station, and most importantly the accuracy required of the ultimate load estimate. The acceptable level of inaccuracy should be considered for each application and a sampling regimen can be designed as needed. Based on the results herein, if one were to find a COV of 5% acceptable, then sampling all three points on the Raccoon River daily would be sufficient and sampling them every seven days would be insufficient. Likewise sampling the

Mississippi River at Baton Rouge every 4 weeks and at Clinton and Thebes every 7 days would be sufficient.

These examples are illustrative only. This experiment could produce more comprehensive, precise results by incorporating data sets longer than 224 days, and high frequency data sets from more stations on more rivers. This analytical framework however, could be implemented if such data sets were available. Perhaps an interested party could install high frequency probes at several key stations along a river for a few years then analyze the data in this fashion to determine the optimal sampling frequencies. If the needs are less frequent than the initial data set, the probe could be adjusted down to conserve battery power, or perhaps manual sampling could be implemented and the high frequency sensors could be reallocated. The computer codes used for data handling in this experiment are included in Appendix B (written in Visual Basic “macro code” for MS Excel).

Overall, high frequency data collection is less important at a station such as Baton Rouge on the Mississippi River than for class 1 streams where the Eulerian dynamics are more rapid. Low frequency monitoring on the smaller streams may miss important hydrologic events and therefore affect the accuracy of the load estimate. Knowledge of the differences in nutrient contribution from each watershed is important as agricultural best management practices are refined and prescribed. Reducing the overall load of nutrients to the Gulf of Mexico requires knowing as much as possible about where they come from in the first place.

## CONCLUSIONS

- ✓ The total nitrogen flux for May and June alone in 2008, from the Mississippi - Atchafalaya River basin was 34% higher than the previous 27 year median (474,000 MT vs. 354,000 MT). For the year as a whole the nitrogen flux was 25% higher than normal (1,750,000 MT vs. 1,400,000 MT), and the phosphorus flux was 50% higher than normal (77,700 MT vs. 51,800 MT).
- ✓ In 2008, nearly one third of the nitrogen (31.2%) and one half of the phosphorus (47.5%) delivered to the Gulf came from just 5% of the Mississippi River basin. The six small watersheds that yielded these nutrients were at the geographical center of the 2008 Midwestern flood (Iowa and Illinois).
- ✓ The 2008 hypoxic zone turned out to be 20,700 km<sup>2</sup> (8,000 mi<sup>2</sup>), which is the second largest since systematic measuring began in 1985
- ✓ The additional nutrient export was theoretically capable of adding 2370 km<sup>2</sup> of area to the annual Gulf of Mexico hypoxic zone (2370 km<sup>2</sup> is 18% of the long term mean size of approximately 13,500 km<sup>2</sup>).
- ✓ Nutrient flux during high flow events was compared to the median flux at monitoring stations across a wide range of drainage areas. As drainage area increased, all nutrient parameters analyzed displayed attenuating yield due to increasing heterogeneity of land use. The highest nutrient flux years were not necessarily the highest discharge years.

- ✓ The accuracy of seasonal load estimates is highly dependent upon the sampling interval used when gathering water quality data. Higher sampling intervals are necessary at stations of smaller drainage area in order to maintain accuracy.
- ✓ To maintain a reasonable level of accuracy, the river stations of smallest drainage area (Sac City in this case) would likely require at least daily sampling, and the largest (Baton Rouge, LA) could likely do with weekly sampling.

The 2008 Midwestern flood swept thousands of tons of valuable nutrients out of Midwestern soils, down the Mississippi River and out into the Gulf of Mexico. Few people realize the magnitude of this invisible export of assets; in 2008 over half of Iowa farmers' nitrogen fertilizer was lost. This event highlighted the "double-edged impact" of agricultural nutrient flux and its associated coastal hypoxia.

As land management practices are assessed and honed to meet Gulf of Mexico hypoxia reduction goals, as well as agricultural production goals, extreme flood events should be considered carefully. As climatologists predict that climate change will likely result in increasing frequency and severity of high-precipitation storm events in the Midwest United States, the risk of repeating events such as occurred in 2008 is expected to grow. Indeed one needs to look no further than Midwestern hydrographs to see the increasing risk: for the five major rivers in Iowa and the upper Mississippi river as a whole, 1993 was the top flow year, followed by 2008, then 1973 or 1983 in position number three in a 68 year record. The period over which these rankings were compiled stretches back to 1942 on average, meaning that the top four flow years have occurred regularly and relatively recently.

The data used for the flux analysis herein is based on the output from LOADEST model runs. The input data used to calibrate each LOADEST run was based on USGS water quality data that was collected monthly, on average. An experiment was designed

to assess the accuracy of load estimates integrated conventionally from data sets of varying frequency. The degree of error in load estimates was found to increase significantly as sampling frequency decreased. Based only on 224 days of data from 2008, sampling at most of the large river stations was found to be too infrequent to convey an accurate load estimate. These results were found from a limited data set, additional calibration data would improve the algorithm as a whole.

## REFERENCES

- Alexander, R., Smith, R., Schwarz, G., Boyer, E., Nolan, J., Brakebill, J. (2008) Differences in phosphorus and nitrogen delivery to the Gulf of Mexico from the Mississippi River basin. *Environmental Science and Technology* 42 822-830
- Aulenbach, B., Buxton, H., Battaglin, W., and Coupe, R. (2008) United States Geological Survey Open File Report 2007-1080; Streamflow and Nutrient Delivery to the Gulf of Mexico. Accessed July 14, 2009 from:  
[http://toxics.usgs.gov/hypoxia/mississippi/flux\\_ests/index.html](http://toxics.usgs.gov/hypoxia/mississippi/flux_ests/index.html)
- Bierman, V.J., Hinz, S.C., Zhu, D.W., Wiseman, W.J., Rabalais, N.N., and Turner, R.E. (1994) A preliminary mass balance model of primary productivity and dissolved oxygen in the Mississippi River Plume/Inner Gulf Shelf Region. *Estuaries and Coasts* 17 (4) 886-899
- Buzicky, G., Randall, G., Hauck, R., and Caldwell, A. (1983) Fertilizer N losses from a tile-drained mollisol as influenced by rate and time of 15-N depleted fertilizer application. *Agronomy Abstracts* 213 American Society of Agronomy.
- CENR (2000) National Science and Technology Council Committee on Environment and Natural Resources. Integrated Assessment of Hypoxia in the Northern Gulf of Mexico. Washington DC
- Cohn, T. A., Caulder, D. L., Gilroy, E. J., Zynjuk, L. D., Summers, R. M. (1992) The Validity of a Simple Statistical Model for Estimating Fluvial Constituent Loads: An Empirical Study Involving Nutrient Loads in Chesapeake Bay. *Water Resources Research* 28 (9) 2353-2363
- DiMarco, S., Jochens, A., and Howard, M. 1997. Louisiana – Texas shelf data report: Current meter moorings April 1992 to December 1994. Texas A&M University Department of Oceanography Technical Report 97-01-T
- Goolsby, D. A., Battaglin, W. A., Thurman, E. M. (1993) Occurrence and Transport of Agricultural Chemicals in the Mississippi River Basin, July through August 1993. U.S. Geological Survey Circular 1120-C.
- Hoefl, R. (1998) Ship Corn, Not Nitrogen down the Mississippi River. Proceedings of the Illinois Agricultural Pesticides Conference, January 6-8, 1998  
Iowa State University. (2010) Cash Corn and Soybean Prices; File A2-11; December 2010. Retrieved January 11, 2011 from  
<http://www.extension.iastate.edu/agdm/crops/pdf/a2-11.pdf>
- Hubbard, L., Kolpin, D. W., Kalkhoff, S. J., Roberson, D.M. (2011) Nutrient and Sediment Concentrations and Corresponding Loads during the Historic June 2008 Flooding in Eastern Iowa. *Journal of Environmental Quality*. 40 166-175
- Kanwar, R., Baker, J., and Laflen, J. (1985) Nitrate Movement Through the Soil Profile in Relation to Tillage System and Fertilizer Application Method. *Transactions of the ASABE* 28 (6), 1802 – 1807

- Libra, R., Wolter, C., Langel, R. (2004) Nitrogen and phosphorus budgets for Iowa and Iowa watersheds, Iowa Department of Natural Resources and Iowa Geological Survey Technical Information Series 47
- Linhart, S.M., and Eash, D.A., 2010, Floods of May 30 to June 15, 2008, in the Iowa and Cedar River basins, eastern Iowa: U.S. Geological Survey Open-File Report 2010–1190
- Mitsch W., Day Jr., J., Gilliam, J., Groffman, P., Hey, D., Randall, G. and Wang, N. (2001) Reducing Nitrogen Loading to the Gulf of Mexico from the Mississippi River Basin: Strategies to Counter a Persistent Ecological Problem. *BioScience*. 51 (5) 373-388
- Putney, M. K. (2010) Using High Frequency Data Collection to Study Nitrate on Clear Creek During High Flow Events. Master's Thesis. University of Iowa, 2010
- Rabalais, N. N. (2008) 'Dead Zone' Again Rivals Record Size. Press Release Louisiana Universities Marine Consortium. 28 July 2008
- Rabalais, N. N., Turner, R. E. (2001) Hypoxia in the northern Gulf of Mexico: Description, causes, and change. *Coastal and estuarine studies; American Geophysical Union*. (58) 1-36
- Rabalais, N. N., Turner, R. E., Justic, D., Dortch, Q., Wiseman, W. (1999) Characterization of Hypoxia. NOAA Coastal Ocean Program Decision Analysis Series 15
- Robertson, D. M., Schwartz, G. E., Saad, D. A., Alexander, R. B. (2009) Incorporating uncertainty into the ranking of sparrow model nutrient yields from Mississippi/Atchafalaya River basin watersheds. *Journal of the American Water Resources Association* 45 (2) 534-549
- Royer, T., Tank, J., David, M. (2004) Transport and Fate of Nitrate in Headwater Agricultural Streams in Illinois. *Journal of Environmental Quality* 33(4),1296-1304.
- Runkel, R.L., Crawford, C.G., and Cohn, T.A. (2004) Load estimator (LOADEST)—A FORTRAN program for estimating constituent loads in streams and rivers: U.S. Geological Survey Techniques and Methods, book 4, chap. A5, p. 69
- Scavia, D., Donnelly, K. (2007) Reassessing Hypoxia Forecasts for the Gulf of Mexico. *Environmental Science and Technology* 41 (23) 8111 – 8117
- Scavia, D., Kelly, E., Hagy III, J. (2006) Nitrogen and water management strategies to reduce nitrate leaching under irrigated maize. *Estuaries and Coasts* 29 (4) 674 – 684
- Scavia, D., Rabalais, N. N., Turner, R.E., Justic, D. and Wiseman Jr., W. (2003) Predicting the response of Gulf of Mexico hypoxia to variations in the Mississippi river nitrogen load. *Limnology and Oceanography* 48, 951–956.
- Schepers, J., Varvel, G., Watts, D. (1995) Nitrogen and Water Management Strategies to Reduce Nitrate Leaching Under Irrigated Maize. *Journal of Contaminant Hydrology* 20 (3-4), 227-239
- Schnoor, J. L. (1996) *Environmental Modeling*. P. 187. John Wiley and Sons. Hoboken, NJ

- Secchi S., Gassman P., Williams J., Babcock B. (2009) Corn-based ethanol production and environmental quality: a case of Iowa and the conservation reserve program. *Environmental Management* 44 (4) 732-744.
- Spalding, R., Exner, M. (1993) Occurrence of Nitrate in Groundwater – A Review. *Journal of Environmental Quality* 22: 392 – 402.
- Stenback, G. A., Crumpton, W. G., Schilling, K. E., Helmers, M. J. (2011) Rating Curve Estimation of Nutrient Loads in Iowa Rivers. *Journal of Hydrology* 396 (1-2) 158-169
- Turner, R.E., Rabalais, N. N., Justic, D. (2006) Predicting summer hypoxia in the northern Gulf of Mexico: Riverine N, P, and Si loading. *Marine Pollution Bulletin* 52 139–148
- Turner, R.E., Rabalais, N. N., (2009) 2009 Hypoxia Forecast, Louisiana State University, June 16, 2009
- [USDA-NASS] United States Department of Agriculture, National Agricultural Statistics Service. (2010) Retrieved December 22, 2010 from [http://quickstats.nass.usda.gov/results/0FB5C4D8-22CD-3971-9C07-0A7CE540A42D?pivot=short\\_desc/](http://quickstats.nass.usda.gov/results/0FB5C4D8-22CD-3971-9C07-0A7CE540A42D?pivot=short_desc/)
- [USDA-NASS] United States Department of Agriculture, National Agricultural Statistics Service. (2010) Retrieved January 11, 2011 from <http://www.apfo.usda.gov/FSA/webapp?area=home&subject=copr&topic=crp-st>
- [USDA-NASS] United States Department of Agriculture, National Agricultural Statistics Service. (2010) Retrieved January 11, 2011 from <http://usda.mannlib.cornell.edu/MannUsda/viewDocumentInfo.do?documentID=1000>



**APPENDIX A - DATA USED TO MAKE  
FIGURES 3-6 THROUGH 3-11**

Table A-1 Total Nitrogen Data

Station	DA	DA	DA	n	non-flood median	non-flood 1st quartile	non-flood 3rd quartile	Top Load	2nd Load	3rd Load	From year	To year	Data Source	
	[mi2]	[km2]	[ha]											[MT N / yr]
Iowa R @ Wapello, IA	12,500	32,375	3,237,485	28	62,700	40,900	91,200	220,000	149,000	114,000	1,978	2,008	no	2
Skunk R @ Augusta, IA	4,312	11,168	1,116,803	24	20,400	13,800	27,000	59,800	49,900	41,400	1,978	2,008	yes	2
Des Moines R @ Keosauqua, IA	14,038	36,358	3,635,825	2	45,900	42,400	49,400	96,000	108,000	52,900	2,004	2,008	no	2
Wapsipinicon R @ DeWitt, IA	2,336	6,050	605,021	7	12,200	9,950	16,700	33,800	26,900	25,700	1,996	2,008	yes	2
Turkey R @ Garber, IA	1,545	4,002	400,153	2	6,100	5,780	6,410	21,700	16,900	13,900	2,004	2,008	no	2
Illinois R @ Valley City, IL	26,743	69,264	6,926,405	29	135,000	108,000	155,000	278,000	196,000	214,000	1,974	2,008	yes	2
Ohio R @ Grand Chain, IL	203,100	526,027	52,602,659	27	513,000	354,000	562,000	751,000	767,000	594,000	1,979	2,008	no	1
Mississippi R @ Clinton, IA	58,600	151,773	15,177,330	28	139,000	108,000	158,000	245,000	211,000	177,000	1,974	2,008	yes	2
UMRB (Miss R @ Thebes minus MO R @ Hermann)	190,700	493,911	49,391,073	27	539,000	450,000	620,000	1,000,000	895,000	1,050,000	1,979	2,008	no	1
Mississippi R + Atchafalaya R @ Gulf of Mexico	1,151,000	2,981,076	298,107,631	26	1,350,000	1,250,000	1,620,000	2,180,000	2,210,000	1,490,000	1,980	2,008	no	1

Table A-2 Nitrate + Nitrite Data

Station	DA [mi2]	DA [km2]	DA [ha]	n [yrs besides top 3]	non- flood median	non- flood 1st quartile	non- flood 3rd quartile	Top Load	2nd Load	3rd Load	Data Source	From Year	To Year	missing interior years?	
								[MT NOx - N / yr]							
Iowa R @ Wapello, IA	12,500	32,375	3,237,485	29	54,700	31,400	92,400	185,000	164,000	145,000	2	1977	2008	no	
Skunk R @ Augusta, IA	4,312	11,168	1,116,803	25	24,400	14,400	37,100	69,800	52,600	56,700	2	1977	2008	yes	
Des Moines R @ Keosauqua, IA	14,038	36,358	3,635,825	2	37,200	34,200	40,300	78,400	87,900	45,300	2	2004	2008	no	
Wapsipinicon R @ DeWitt, IA	2,336	6,050	605,021	8	13,600	9,790	17,900	28,300	39,700	35,600	2	1993	2008	yes	
Turkey R @ Garber, IA	1,545	4,002	400,153	2	5,150	4,960	5,340	15,400	13,200	10,600	2	2004	2008	no	
Illinois R @ Valley City, IL	26,743	69,264	6,926,405	29	102,000	75,700	122,000	229,000	179,000	161,000	2	1977	2008	no	
Ohio R @ Grand Chain, IL	203,100	526,027	52,602,659	27	117,000	89,100	137,000	181,000	216,000	149,000	1	1979	2008	no	
Mississippi R @ Clinton, IA	58,600	151,773	15,177,330	24	101,000	75,000	125,000	276,000	193,000	208,000	2	1977	2008	yes	
Mississippi R @ Grafton, IL	171,300	443,665	44,366,496	29	122,000	86,900	147,000	262,000	210,000	196,000	1	1975	2008	yes	
UMRB (Miss R @ Thebes minus MO R @ Hermann)	190,700	493,911	49,391,073	27	132,000	106,000	161,000	277,000	237,000	222,000	2	1979	2008	no	
Mississippi R + Atchafalaya R @ Gulf of Mexico	1,151,000	2,981,076	298,107,631	27	323,000	293,000	376,000	595,000	507,000	427,000	1	1979	2008	no	
Data Sources:	1 = USGS O-F R 2007-1080, B. Aulenbach		2 = USGS data, Processed by A. Gwinnup via LOADEST												

Table A-3 Total Kjeldahl Nitrogen Data

Station	DA	DA	DA	DA	n	non-flood median	non-flood 1st quartile	non-flood 3rd quartile	Top Load	2nd Load	3rd Load	From year	To year	missing interior years?	Data Source
	[mi2]	[km2]	[ha]	[ha]	[yrs besides top 3]				[MT TKN - N / yr]						
Iowa R @ Wapello, IA	12,500	32,375	3,237,485	3,237,485	23	12,500	9,300	17,400	39,800	23,800	17,900	1,978	2,003	no	2
Skunk R @ Augusta, IA	4,312	11,168	1,116,803	1,116,803	20	5,200	3,190	8,280	18,500	9,270	10,700	1,978	2,007	yes	2
Des Moines R @ Keosauqua, IA	14,038	36,358	3,635,825	3,635,825	-	-	-	-	-	-	-	-	-	-	2
Wapsipinicon R @ DeWitt, IA	2,336	6,050	605,021	605,021	3	2,250	2,220	2,270	3,280	3,640	3,960	1,996	2,007	yes	2
Turkey R @ Garber, IA	1,545	4,002	400,153	400,153	-	-	-	-	-	-	-	-	-	-	2
Illinois R @ Valley City, IL	26,743	69,264	6,926,405	6,926,405	26	28,100	23,500	35,600	29,300	33,800	39,400	1,977	2,008	yes	2
Ohio R @ Grand Chain, IL	203,100	526,027	52,602,659	52,602,659	27	64,200	42,700	77,200	92,300	64,200	67,500	1,979	2,008	no	1
Mississippi R @ Clinton, IA	58,600	151,773	15,177,330	15,177,330	23	18,500	16,100	22,300	28,500	31,100	18,800	1,975	2,008	yes	2
Mississippi R @ Grafton, IL	171,300	443,665	44,366,496	44,366,496	29	49,600	39,400	57,300	73,700	83,200	108,000	1,975	2,008	yes	1
UMRB (Miss R @ Thebes minus MO R @ Hermann)	190,700	493,911	49,391,073	49,391,073	27	51,800	43,100	66,400	88,300	89,800	160,000	1,979	2,008	no	2
Mississippi R + Atchafalaya R @ Gulf of Mexico	1,151,000	2,981,076	298,107,631	298,107,631	26	170,000	159,000	237,000	199,000	299,000	164,000	1,980	2,008	no	1
Data Sources:	1 = USGS O-F R 2007-1080, B. Aulenbach														
	2 = USGS data, Processed by A. Gwinnup via LOADEST														

Table A-4 Total Unfiltered Phosphorus Data

Station	DA	DA	DA	DA	n	non-flood median	non-flood 1st quartile	non-flood 3rd quartile	Top Load	2nd Load	3rd Load	From year		Data Source	
												To year	Year?		
	[mi2]	[km2]	[ha]	[ha]	[yrs besides top 3]				[MT P / yr]						
Iowa R @ Wapello, IA	12,500	32,375	3,237,485	29	2,580	1,780	3,540	9,740	7,800	4,890	1,977	2,008	no	2	
Skunk R @ Augusta, IA	4,312	11,168	1,116,803	25	1,160	623	1,670	5,600	4,280	2,660	1,977	2,008	yes	2	
Des Moines R @ Keosauqua, IA	14,038	36,358	3,635,825	2	4,750	4,660	4,850	2,060	1,800	1,390	2,004	2,008	no	2	
Wapsipinicon R @ DeWitt, IA	2,336	6,050	605,021	7	467	355	632	1,150	700	847	1,996	2,008	yes	2	
Turkey R @ Garber, IA	1,545	4,002	400,153	2	175	162	189	1,250	721	1,390	2,004	2,008	no	2	
Illinois R @ Valley City, IL	26,743	69,264	6,926,405	29	7,570	6,590	8,580	13,700	17,500	10,000	1,977	2,008	no	2	
Ohio R @ Grand Chain, IL	203,100	526,027	52,602,659	27	15,800	10,800	20,300	30,300	18,100	23,300	1,979	2,008	no	1	
Mississippi R @ Clinton, IA	58,600	151,773	15,177,330	23	2,920	2,620	3,290	3,980	4,530	3,980	1,975	2,008	yes	2	
Mississippi R @ Grafton, IL	171,300	443,665	44,366,496	29	10,900	8,180	13,100	11,600	9,270	4,160	1,975	2,008	yes	1	
UMRB (Miss R @ Thebes minus MO R @ Hermann)	190,700	493,911	49,391,073	27	13,100	11,000	15,200	30,000	27,900	9,270	1,979	2,008	no	2	
Mississippi R + Atchafalaya R @ Gulf of Mexico	1,151,000	2,981,076	298,107,631	27	49,600	47,800	58,000	61,700	57,700	66,400	1,968	2,008	yes	1	
Data Sources:	1 = USGS O-F-R 2007-1080, B. Aulenbach													2 = USGS data, Processed by A. Gwinnup via LOADEST	

Table A-5 Dissolved Silica Data

Station	DA [mi2]	DA [km2]	DA [ha]	n [yrs besides top 3]	non- flood median	non-flood quartile			Top Load [MT SiO <sub>2</sub> / yr]	2nd Load	3rd Load	From year	To year	missing interior years?	Data Source
						1st	3rd	quartile							
Iowa R @ Wapello, IA	12,500	32,375	3,237,485	28	99,700	65,600	187,000	525,000	365,000	287,000	1,977	2,008	yes	2	
Skunk R @ Augusta, IA	4,312	11,168	1,116,803	25	36,600	25,500	50,800	124,000	89,700	84,300	1,977	2,008	yes	2	
Des Moines R @ Keosauqua, IA	14,038	36,358	3,635,825	2	63,600	58,700	68,500	236,000	205,000	94,900	2,004	2,008	no	2	
Wapsipinicon R @ DeWitt, IA	2,336	6,050	605,021	7	14,700	11,800	24,100	57,000	86,800	64,200	1,996	2,008	yes	2	
Turkey R @ Garber, IA	1,545	4,002	400,153	2	6,100	5,740	6,450	24,000	21,100	11,700	2,004	2,008	no	2	
Illinois R @ Valley City, IL	26,743	69,264	6,926,405	17	157,000	116,000	170,000	369,000	253,000	255,000	1,977	2,008	yes	2	
Ohio R @ Grand Chain, IL	203,100	526,027	52,602,659	27	467,000	368,000	610,000	814,000	588,000	675,000	1,979	2,008	no	1	
Mississippi R @ Clinton, IA	58,600	151,773	15,177,330	22	169,000	127,000	220,000	196,000	291,000	330,000	1,975	2,008	yes	2	
Mississippi R @ Grafton, IL	171,300	443,665	44,366,496	29	316,000	204,000	405,000	982,000	624,000	577,000	1,975	2,008	yes	1	
UMRB (Miss R @ Thebes minus MO R @ Hermann)	190,700	493,911	49,391,073	18	326,000	268,000	394,000	694,000	668,000	537,000	1,979	2,008	yes	2	
Mississippi R + Atchafalaya R @ Gulf of Mexico	1,151,000	2,981,076	298,107,631	26	1,530,000	1,320,000	1,760,000	2,650,000	2,120,000	1,930,000	1,980	2,008	no	1	
Data Sources:	1 = USGS O-F R 2007-1080, B. Aulenbach														
	2 = USGS data, Processed by A. Gwinnup via LOADEST														

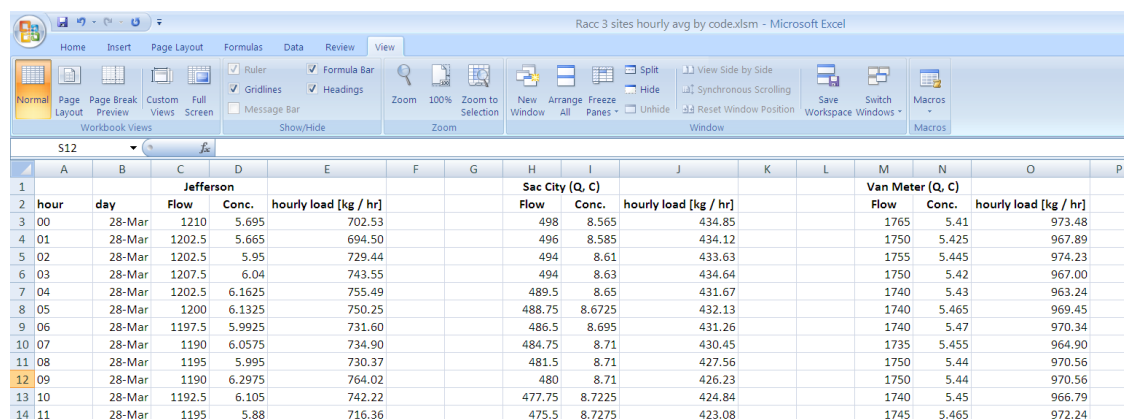
Table A-6 Total Suspended Solids Data

Station	DA	DA	DA	n	non-flood			Top Load	2nd Load	3rd Load	From year	To year	missing interior years?
	[mi2]	[km2]	[ha]		median	1st quartile	non-flood 3rd quartile						
Iowa R @ Wapello, IA	12,500	32,375	3,237,485	28	2,310,000	1,280,000	4,120,000	12,300,000	5,740,000	3,370,000	1978	2008	no
Skunk R @ Augusta, IA	4,312	11,168	1,116,803	29	1,730,000	852,000	3,570,000	19,700,000	4,040,000	5,040,000	1977	2008	no
Des Moines R @ Keosauqua, IA	14,038	36,358	3,635,825	2	1,090,000	859,000	1,310,000	6,330,000	3,700,000	2,680,000	2004	2008	no
Wapsipinicon R @ DeWitt, IA	2,336	6,050	605,021	11	478,000	265,000	528,000	1,090,000	933,000	615,000	1978	2008	yes
Turkey R @ Garber, IA	1,545	4,002	400,153	7	269,000	186,000	574,000	2,570,000	920,000	1,090,000	1978	2008	yes
Illinois R @ Valley City, IL	26,743	69,264	6,926,405	26	5,050,000	3,880,000	7,200,000	7,370,000	12,000,000	8,080,000	1977	2008	yes
Ohio R @ Grand Chain, IL	203,100	526,027	52,602,659	26	31,000,000	19,900,000	43,000,000	43,700,000	48,100,000	43,600,000	1980	2008	no
Mississippi R @ Clinton, IA	58,600	151,773	15,177,330	24	3,710,000	2,460,000	4,300,000	8,790,000	7,490,000	5,100,000	1977	2008	yes
UMRB (Miss R @ Thebes minus MO R @ Hermann)	190,700	493,911	49,391,073	19	15,500,000	13,100,000	25,700,000	46,000,000	46,900,000	40,000,000	-	-	-
Mississippi R + Atchafalaya R @ Gulf of Mexico	1,151,000	2,981,076	298,107,631	26	149,000,000	125,000,000	199,000,000	340,000,000	176,000,000	124,000,000	1980	2008	yes
Data Sources:	1 = USGS O-FR 2007-1080, B. Aulenbach      2 = USGS data, Processed by A. Gwinnup via LOADFEST												

## APPENDIX B – COMPUTER CODE FOR FREQUENCY ANALYSIS

Below are programming codes for resampling data sets to define acceptable sampling frequencies for surface water quality monitoring. The actual method is simple, but working iteratively through high frequency data sets requires computer processing. The codes are designed to be implemented as macros in Microsoft Excel, some code-level input is required as all data sets vary in size. In order to run this code, open MS Excel and save a new spreadsheet as a “macro enabled” spreadsheet (\*.xlsm). Rename one tab “INPUT” and one tab “RESULTS”. On the “View” tab, click “Macros”, then enter the macro subroutine name “freqResampler” and click “Create”. A Visual Basic compiler will open, copy and paste the following code into the code window.

Before running the macro, set up the INPUT and RESULTS sheets. This can be done in the same manner as Figures B-1 and B-2 below, or any way you like, but the column and row numbers in the code must match your layout.



	A	B	Jefferson			Sac City (Q, C)			Van Meter (Q, C)		
1	hour	day	Flow	Conc.	hourly load [kg / hr]	Flow	Conc.	hourly load [kg / hr]	Flow	Conc.	hourly load [kg / hr]
2	00	28-Mar	1210	5.695	702.53	498	8.565	434.85	1765	5.41	973.48
4	01	28-Mar	1202.5	5.665	694.50	496	8.585	434.12	1750	5.425	967.89
5	02	28-Mar	1202.5	5.95	729.44	494	8.61	433.63	1755	5.445	974.23
6	03	28-Mar	1207.5	6.04	743.55	494	8.63	434.64	1750	5.42	967.00
7	04	28-Mar	1202.5	6.1625	755.49	489.5	8.65	431.67	1740	5.43	963.24
8	05	28-Mar	1200	6.1325	750.25	488.75	8.6725	432.13	1740	5.465	969.45
9	06	28-Mar	1197.5	5.9925	731.60	486.5	8.695	431.26	1740	5.47	970.34
10	07	28-Mar	1190	6.0575	734.90	484.75	8.71	430.45	1735	5.455	964.90
11	08	28-Mar	1195	5.995	730.37	481.5	8.71	427.56	1750	5.44	970.56
12	09	28-Mar	1190	6.2975	764.02	480	8.71	426.23	1750	5.44	970.56
13	10	28-Mar	1192.5	6.105	742.22	477.75	8.7225	424.84	1740	5.45	966.79
14	11	28-Mar	1195	5.88	716.36	475.5	8.7275	423.08	1745	5.465	972.24

Figure B-1. INPUT data spreadsheet layout



METHOD	RUN #	LOAD [MT - N]													
Hourly Q x hourly C	resampled every ___ hours	11,680	5,353	19,696	ERROR?	rows per sum	rows per sum	rows per sum	hours per sum	hours per sum	hours per sum				
2	1	11,681	5,352	19,674		2688	2688	2688	5376	5376	5376				
6	2	11,679	5,353	19,717		2688	2688	2688	5376	5376	5376				
6	1	11,681	5,356	19,701		896	896	896	5376	5376	5376				
6	2	11,687	5,354	19,703		896	896	896	5376	5376	5376				
6	3	11,684	5,350	19,718		896	896	896	5376	5376	5376				
6	4	11,678	5,348	19,778		896	896	896	5376	5376	5376				
6	5	11,678	5,351	19,804		896	896	896	5376	5376	5376				
6	6	11,673	5,357	19,671		896	896	896	5376	5376	5376				
12	1	11,713	5,356	19,796		448	448	448	5376	5376	5376				
12	2	11,713	5,355	19,782		448	448	448	5376	5376	5376				
12	3	11,694	5,354	19,814		448	448	448	5376	5376	5376				
12	4	11,672	5,350	19,802		448	448	448	5376	5376	5376				

Figure B-2. RESULTS spreadsheet layout

Sub freqResampler()

Worksheets("RESULTS").Activate

Dim rowLoop As Integer

Dim colLoop As Integer

Dim increment As Integer

Dim startpoint As Integer

Dim load As Double

Dim pointLoad As Double

Dim count As Integer

Dim writeRow As Integer

Dim hourlyInterval As Integer

Dim initOffset As Integer

Dim begrow As Integer

Dim firstrow As Integer

Dim outerLoop As Integer

Dim endrow As Integer

" this code displays the terminal message box

Dim Msg, completeMsg, incompleteMsg, Style, Title

completeMsg = "Last cell was calculated successfully"

incompleteMsg = "Last cell was NOT calculated"

Style = vbOK + vbCritical

Title = "Re-sampling code execution report"

INPUT REQUIRED

' the following 2 values pertain to the input data

' worksheet's first and last rows of input data

firstrow = 3

endrow = 5378

' the following 2 values pertain to the output

' worksheet's first and last rows (the "outer loop")

firstoutsidelooprow = 889

endoutsidelooprow = 4920

INPUT REQUIRED

' Define message

' Define message.

' Define buttons.

' Define title.

```

'beginning of operating code
For i = firstoutsidelooprow To endoutsidelooprow
hourlyInterval = Cells(i, 1).Value
initOffset = (Cells(i, 2).Value - 1)
writeRow = i
begrow = firstrow + initOffset
For colLoop = 5 To 15 Step 5
' 5, 10, and 15 are the hourly load columns on the input data worksheet
load = 0
count = 0
For rowLoop = begrow To endrow Step hourlyInterval
pointLoad = Worksheets("INPUT").Cells(rowLoop,colLoop).Value
intervalLoad = pointLoad * hourlyInterval
load = load + intervalLoad
count = count + 1
Next rowLoop
load = load * 0.001 ' converts sum to metric tons
If colLoop = 5 Then
Cells(writeRow, 3).Value = load
Cells(writeRow, 8).Value = count
Cells(writeRow, 11).Value = (count * hourlyInterval)
ElseIf colLoop = 10 Then
Cells(writeRow, 4).Value = load
Cells(writeRow, 9).Value = count
Cells(writeRow, 12).Value = (count * hourlyInterval)
ElseIf colLoop = 15 Then
Cells(writeRow, 5).Value = load
Cells(writeRow, 10).Value = count
Cells(writeRow, 13).Value = (count * hourlyInterval)
Else
Cells(writeRow, 7).Value = "load write error"
Cells(writeRow, 10).Value = count
Cells(writeRow, 13).Value = (count * hourlyInterval)
End If
Next colLoop
Next i
If ((rowLoop > endrow) And colLoop = 20 And i = (endoutsidelooprow + 1)) Then
Msg = completeMsg
Else
Msg = incompleteMsg
End If
Response = MsgBox(Msg, Style, Title)
End Sub

```

Below are programming codes for producing hourly means from 15 minute data sets. This specific code was written for a sheet containing data from 3 stations for one year. Follow the directions above for setting up the macro, also adjust sheet names as

necessary, this code uses an input sheet named “08\_cleaned\_and\_synched” and an output sheet named “reduced\_to\_Hourly”.

```

Sub hourly_avger()
Worksheets("reduced_to_Hourly").Activate
Dim jQarray(3) As Variant
Dim jCarray(3) As Variant
Dim sQarray(3) As Variant
Dim sCarray(3) As Variant
Dim vQarray(3) As Variant
Dim vCarray(3) As Variant
Dim jqm As Double
Dim jqc As Integer
Dim jq As Double
Dim sqm As Double
Dim sqc As Integer
Dim sq As Double
Dim vqm As Double
Dim vqc As Integer
Dim vq As Double
Dim jcm As Double
Dim jcc As Integer
Dim jc As Double
Dim scm As Double
Dim scc As Integer
Dim sc As Double
Dim vcm As Double
Dim vcc As Integer
Dim vc As Double
Dim row As Integer
Dim i As Long
Dim j As Integer
Dim k As Integer
Dim daymo As Date
Dim hour As String
Dim holdhr As String
Dim hloddt As Date
Dim imo As Integer
Dim iday As Integer
Dim da As Integer
Dim mo As Integer
Dim lefthr As String
For row = 2 To 50
daymo = Cells(row, 2).Value
da = Day(daymo)
mo = Month(daymo)
hour = Cells(row, 1).Value
For i = 4 To 195 Step 4
holdhr = Worksheets("08_cleaned_and_synched").Cells(i, 1).Value
holddt = Worksheets("08_cleaned_and_synched").Cells(i, 2).Value
imo = Month(holddt)

```

```

iday = Day(holddt)
lefthr = Left(holdhr, 2)
If (iday = da And imo = mo And lefthr = hour) Then
For j = 0 To 3
If Worksheets("08_cleaned_and_synched").Cells((i + j), 6).Value = "x" Then
jQarray(j) = Empty
Else
jQarray(j) = Worksheets("08_cleaned_and_synched").Cells((i + j), 6).Value
End If
If Worksheets("08_cleaned_and_synched").Cells((i + j), 7).Value = "x" Then
jCarray(j) = Empty
Else
jCarray(j) = Worksheets("08_cleaned_and_synched").Cells((i + j), 7).Value
End If
If Worksheets("08_cleaned_and_synched").Cells((i + j), 12).Value = "x" Then
sQarray(j) = Empty
Else
sQarray(j) = Worksheets("08_cleaned_and_synched").Cells((i + j), 12).Value
End If
If Worksheets("08_cleaned_and_synched").Cells((i + j), 13).Value = "x" Then
sCarray(j) = Empty
Else
sCarray(j) = Worksheets("08_cleaned_and_synched").Cells((i + j), 13).Value
End If
If Worksheets("08_cleaned_and_synched").Cells((i + j), 17).Value = "x" Then
vQarray(j) = Empty
Else
vQarray(j) = Worksheets("08_cleaned_and_synched").Cells((i + j), 17).Value
End If
If Worksheets("08_cleaned_and_synched").Cells((i + j), 18).Value = "x" Then
vCarray(j) = Empty
Else
vCarray(j) = Worksheets("08_cleaned_and_synched").Cells((i + j), 18).Value
End If
Next j
jqm = Application.WorksheetFunction.Sum(jQarray(0), jQarray(1), jQarray(2),
jQarray(3))
jqc = Application.WorksheetFunction.count(jQarray)
jq = jqm / jqc
Cells(row, 3).Value = jq
jcm = Application.WorksheetFunction.Sum(jCarray(0), jCarray(1), jCarray(2),
jCarray(3))
jcc = Application.WorksheetFunction.count(jCarray)
jc = jcm / jcc
Cells(row, 4).Value = jc
sqm = Application.WorksheetFunction.Sum(sQarray(0), sQarray(1), sQarray(2),
sQarray(3))
sqc = Application.WorksheetFunction.count(sQarray)
sq = sqm / sqc
Cells(row, 5).Value = sq
scm = Application.WorksheetFunction.Sum(sCarray(0), sCarray(1), sCarray(2),
sCarray(3))
scc = Application.WorksheetFunction.count(sCarray)
sc = scm / scc

```

```
Cells(row, 6).Value = sc
vqm = Application.WorksheetFunction.Sum(vQarray(0), vQarray(1), vQarray(2),
vQarray(3))
vqc = Application.WorksheetFunction.count(vQarray)
vq = vqm / vqc
Cells(row, 7).Value = vq
vcm = Application.WorksheetFunction.Sum(vCarray(0), vCarray(1), vCarray(2),
vCarray(3))
vcc = Application.WorksheetFunction.count(vCarray)
vc = vcm / vcc
Cells(row, 8).Value = vc
End If
Next i
Next row
End Sub
```